-Supporting Information-

Regioselective Synthesis of Multifunctional Dibenzo-Heterocyclic Dihydrophenazine Derivatives: Tunable Excited-State Structural Relaxation and Efficient Red OLED Host Materials

Kai Kang,[a] Chunyan Zhang,[a] Yi Chen,[b] Jinhai Huang,[b] Xin Jin,[*a] Zhiyun Zhang[a]

[a]Key Laboratory for Advanced Materials and Joint International Research Laboratory of Precision Chemistry and Molecular Engineering, Feringa Nobel Prize Scientist Joint Research Centre, Frontiers Science Center for Materiobiology and Dynamic Chemistry, East China University of Science & Technology, Shanghai 200237, China

[b]Shanghai Taoe Chemical Technology Co., Ltd, Shanghai 200030, P. R. China

*Correspondence to: xin_jin@ecust.edu.cn (Xin Jin)

Table of Content

1. Materials and general methods

Synthesis and characterization. All reagents and solvents were purchased from commercial sources and were of analytical grade. ^{1}H and ^{13}C NMR spectra were recorded on a Bruker AM 400 spectrometer and Ascend 600 spectrometer with tetramethylsilane as the internal standard, operating at 400/600 MHz and 101/151 MHz, respectively. The following abbreviations were used to explain multiplicities: s = singlet, d = doublet, t = triplet, q = quartet, m = multiplet, br = broad. High-resolution mass spectrometry (HRMS) spectra were recorded with a Direct Analysis in Real Time (DART) mass spectroscope. The X-ray diffraction intensity data were collected at 273 K or 200 K on a Rigaku RAXIS RAPID IP imaging plate system with MoKα radiation (λ = 0.71073 Å). The CIF files for the crystallographic data have been deposited in the Cambridge Crystallographic Data Centre, and the CCDC numbers are shown in Table S1. (See https://www.ccdc.cam.ac.uk/)

Spectroscopic measurements. The steady-state absorption and emission spectra were used a Hitachi (U-3310) spectrophotometer and an Edinburgh Instruments Fluorescence Spectrometer FLS1000 fluorimeter to acquire, respectively. Nanosecond time-resolved studies were performed with an Edinburgh Instruments Fluorescence Spectrometer FLS1000 time-correlated single photon-counting (TCSPC) system. The instrumental response function (IRF) was determined from the scattering signal of a silica water solution. Fitting was carried out using Fluoracle software employing single exponential decay functions. All the spectroscopic pure reagents used were obtained through distillation column rectification.

Femtosecond transient absorption (TA) spectroscopy. The femtosecond transient absorption setup used for this study is based on a regenerative amplified Ti:sapphire laser system from Coherent (800 nm, 35 fs, 6 mJ·pulse^{-1}, and 1 KHz repetition rate), nonlinear frequency mixing techniques and the Femto-TA100 spectrometer (Time-Tech Spectra). Briefly, the 800 nm output pulse from the regenerative amplifier was

split in two parts with a 50% beam splitter. The transmitted part was used to pump a TOPAS Optical Parametric Amplifier (OPA) which generates a laser pulse (340 nm) as pump beam. The reflected 800 nm beam was split again into two parts. One part with less than 10% was attenuated with a neutral density filter and focused into a 2.5 mm thick CaF_2 window to generate a white-light continuum (WLC) from 300 nm to 700 nm used for probe beam.

Computational methodology. For all titled molecules, the geometry optimization and energy calculation of the ground state and the excited state structures with related photophysical properties were realized by Density Functional Theory (DFT) method and time-dependent DFT (TD-DFT) method, respectively. Using (TD) CAM-B3LYP function alone with def2-SVP basis set using the IEFPCM model to simulate the cyclohexane environment [1-6] with using the single crystal structure as the initial conformation. The CFF value atomic Color-coded, HOMO-LUMO and reduced density gradient (RDG) iso-surfaces maps of were rendered by means of Visual Molecular Dynamics (VMD) software based on the files exported by Multiwfn.[7] All theoretical calculations were performed using the Gaussian 16 program.

2. Synthesis details

Condition 1

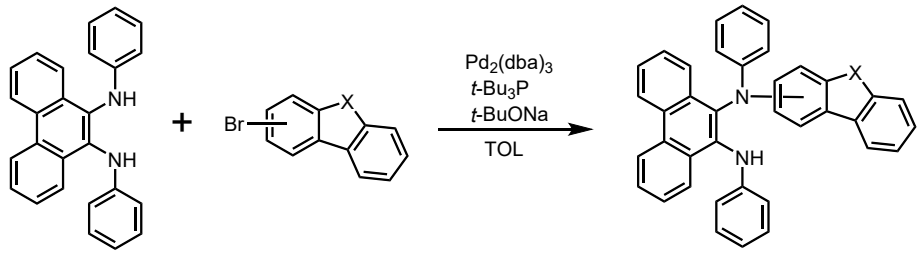

PHNH **R** **I**

General procedure for the synthesis of **I-**x. **PHNH** (1g, 2.78 mmol), **R-**x (2.78 mmol), $Pd_2(dba)_3$ (30 mg, 0.03 mmol), tri-tert-butylphosphine tetrafluoroborate (35 mg, 0.1 mmol) and sodium tert-butoxide (550 mg, 5.7 mmol) were added to a Schlenk flask containing a stir bar. After evacuating and refilling with nitrogen (three cycles), anhydrous toluene (5 mL) was added to the Schlenk flask, heated to reflux and stirred overnight. After cooling to room temperature, diluted and extracted with EtOAc (25 mL), washed with brine and the organic ingredients were dried over Na_2SO_4 for 15 min and removed by a rotatory evaporation. The crude product was purified by column chromatography to desire **I-**x.

Synthesis of *N^9,N^{10}-diphenyl-N^9-(9-phenyl-9H-carbazol-2-yl)phenanthrene-9,10-diamine* (**I-**a)

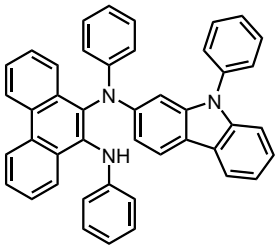

Purified by flash column chromatography on silica gel (PE/DCM = 8:1-2:1) to afford **I-**a as a white solid (1.12g, 67%). ^{1}H NMR (400 MHz, $CDCl_3$-*d*): δ 8.77 (t, *J* = 9.0 Hz, 2H), 8.05 – 7.96 (m, 3H), 7.88 (d, *J* = 8.5 Hz, 1H), 7.69 (m, 1H), 7.60 (m, 1H), 7.53 – 7.42 (m, 4H), 7.38 – 7.30 (m, 5H), 7.24 (m, 1H), 7.14 (m, 5H), 7.04 (m, 1H), 6.97 – 6.86 (m, 3H), 6.66 (t, *J* = 7.3 Hz, 1H), 6.43 – 6.36 (m, 2H). ^{13}C NMR (101 MHz, $CDCl_3$-*d*): δ 146.29, 145.90, 145.77, 141.08, 138.88, 135.73, 135.40, 133.41, 131.16, 130.83,

130.44, 129.95, 129.56, 128.73, 127.57, 127.20, 126.82, 126.24, 125.67, 124.97, 124.39, 123.02, 122.95, 122.63, 122.39, 122.24, 121.01, 120.77, 119.50, 117.89, 115.67, 113.45; HRMS DART (m/z) $[M+H]^+$: calcd. for $C_{44}H_{32}N_3$: 602.2591; found: 602.2575.

Synthesis of *N^9-(dibenzo[b,d]thiophen-3-yl)-N^9,N^{10}-diphenylphenanthrene-9,10-diamine* (**I-**b)

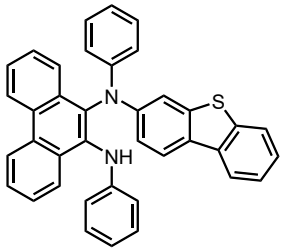

Purified by flash column chromatography on silica gel (PE/DCM = 10:1-5:1) to afford **I-**b as a white solid (1.13g, 75%). ^{1}H NMR (400 MHz, $CDCl_3$-*d*): δ 8.80 (t, *J* = 8.0 Hz, 2H), 8.04 (t, *J* = 8.6 Hz, 2H), 7.98 (m, 1H), 7.89 (d, *J* = 8.7 Hz, 1H), 7.78 – 7.69 (m, 2H), 7.67 – 7.60 (m, 1H), 7.57 – 7.44 (m, 3H), 7.43 – 7.34 (m, 2H), 7.27 – 7.13 (m, 5H), 6.97 (m, 3H), 6.67 (t, *J* = 7.3 Hz, 1H), 6.47 (d, *J* = 7.9 Hz, 2H); ^{13}C NMR (101 MHz, $CDCl_3$-*d*): δ 146.29, 145.90, 145.77, 141.08, 138.88, 135.73, 135.40, 133.41, 131.16, 130.83, 130.44, 129.95, 129.56, 128.73, 127.57, 127.20, 126.82, 126.24, 125.67, 124.97, 124.39, 123.02, 122.95, 122.63, 122.39, 122.24, 121.01, 120.77, 119.50, 117.89, 115.67, 113.45; HRMS DART (m/z) $[M+H]^+$: calcd. for $C_{38}H_{27}N_2S$: 543.1889; found: 543.1871.

Synthesis of *N^9,N^{10}-diphenyl-N^9-(9-phenyl-9H-carbazol-4-yl)phenanthrene-9,10-diamine* (**I-**c)

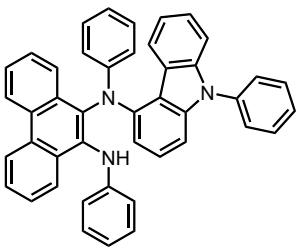

Purified by flash column chromatography on silica gel (PE/DCM = 8:1-2:1) to afford **I-**c as a white solid (1.20g, 72%). ^{1}H NMR (400 MHz, $CDCl_3$-*d*): δ 8.80 (t, *J* = 8.6 Hz,

2H), 8.20 (d, *J* = 8.2 Hz, 1H), 7.89 (d, *J* = 8.3 Hz, 1H), 7.73 – 7.34 (m, 12H), 7.16 (m, 2H), 7.05 (t, *J* = 7.8 Hz, 2H), 6.99 – 6.89 (m, 3H), 6.85 (t, *J* = 7.3 Hz, 1H), 6.79 – 6.43 (m, 4H), 6.16 (s, 1H), 5.43 (d, *J* = 84.4 Hz, 2H); ^{13}C NMR (101 MHz, $CDCl_3$-*d*): δ 147.69, 145.19, 142.28, 141.30, 139.17, 137.45, 130.35, 130.32, 129.87, 129.77, 129.67, 129.53, 127.74, 127.34, 126.86, 126.70, 126.67, 126.03, 125.86, 125.61, 123.15, 122.99, 122.81, 121.25, 120.19, 118.85, 117.01, 115.17, 109.32, 106.62; HRMS DART (m/z) $[M+H]^+$: calcd. for $C_{44}H_{32}N_3$: 602.2591; found: 602.2573.

Synthesis of *N^9-(dibenzo[b,d]thiophen-1-yl)-N^9,N^{10}-diphenylphenanthrene-9,10-diamine* (**I-**d)

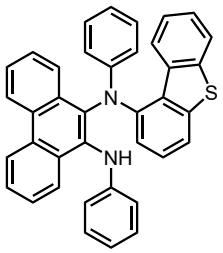

Purified by flash column chromatography on silica gel (PE/DCM = 10:1-3:1) to afford **I-**d as a white solid (1.37g, 91%).^{1}H NMR (400 MHz, $CDCl_3$-*d*): δ 8.79 (m, 2H), 8.09 (d, *J* = 8.3 Hz, 1H), 7.91 (m, 3H), 7.77 – 7.35 (m, 6H), 7.26 (d, *J* = 7.6 Hz, 1H), 7.22 – 6.93 (m, 5H), 6.81 (t, *J* = 7.3 Hz, 1H), 6.73 – 6.66 (m, 2H), 6.59 (t, *J* = 7.6 Hz, 2H), 6.49 (t, *J* = 7.3 Hz, 1H), 5.50 (d, *J* = 7.9 Hz, 1H), 5.32 (s, 2H); ^{13}C NMR (101 MHz, $CDCl_3$-*d*): δ 148.03, 144.94, 141.15, 140.98, 140.04, 136.44, 134.69, 133.42, 131.30, 130.78, 130.58, 130.36, 129.80, 129.73, 129.51, 128.82, 127.79, 127.46, 127.09, 126.98, 126.85, 126.23, 126.17, 126.05, 125.82, 125.51, 124.54, 124.02, 123.17, 122.76, 122.40, 120.07, 119.92, 119.05, 117.66, 115.15, 114.75, 114.60; HRMS DART (m/z) $[M+H]^+$: calcd. for $C_{38}H_{27}N_2S$: 543.1889; found: 543.1873.

Synthesis of *N^9-(9,9-dimethyl-9H-fluoren-4-yl)-N^9,N^{10}-diphenylphenanthrene-9,10-diamine* (**I-**e)

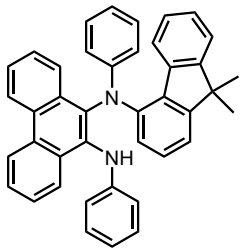

Purified by flash column chromatography on silica gel (PE/DCM = 10:1-4:1) to afford **I-**e as a white solid (1.36g, 89%). ^{1}H NMR (400 MHz, $CDCl_3$-*d*): δ 8.78 (t, *J* = 8.2 Hz, 2H), 8.06 (d, *J* = 8.3 Hz, 1H), 7.92 – 7.78 (m, 1H), 7.72 – 7.39 (m, 5H), 7.32 (d, *J* = 7.6 Hz, 1H), 7.10 (m, 6H), 6.81 (m, 2H), 6.72 – 6.19 (m, 5H), 5.74 (d, *J* = 7.9 Hz, 2H), 1.48 (s, 3H), 1.13 (s, 3H); ^{13}C NMR (101 MHz, $CDCl_3$-*d*): δ 155.78, 154.30, 147.93, 145.16, 139.02, 130.96, 130.49, 130.23, 129.84, 129.66, 128.89, 128.63, 128.11, 127.20, 127.11, 126.87, 126.61, 126.13, 125.95, 125.58, 123.78, 123.03, 122.82, 122.23, 119.42, 117.04, 116.00, 114.38, 46.53, 28.18, 26.28; HRMS DART (m/z) $[M+H]^+$: calcd. for $C_{41}H_{33}N_2$: 553.2638; found: 553.2620.

Synthesis of *N^9-(dibenzo[b,d]furan-1-yl)-N^9,N^{10}-diphenylphenanthrene-9,10-diamine* (**I-**f)

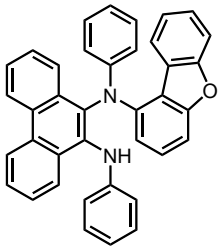

Purified by flash column chromatography on silica gel (PE/DCM = 10:1-4:1) to afford **I-**f as a white solid (1.20g, 82%). ^{1}H NMR (400 MHz, $CDCl_3$-*d*): δ 8.80 (m, 2H), 8.08 (d, *J* = 8.2 Hz, 1H), 7.95 (d, *J* = 8.3 Hz, 1H), 7.67 (m, 2H), 7.59 (d, *J* = 8.3 Hz, 1H), 7.47 (m, 3H), 7.14 (m, 4H), 7.05 (t, *J* = 7.6 Hz, 1H), 6.99 – 6.82 (m, 4H), 6.73 (t, *J* = 7.8 Hz, 3H), 6.58 (t, *J* = 7.3 Hz, 1H), 5.84 (d, *J* = 6.7 Hz, 2H); ^{13}C NMR (101 MHz, $CDCl_3$-*d*): δ 157.09, 156.05, 147.01, 145.12, 139.63, 136.03, 134.17, 131.14, 130.56, 130.37, 129.96, 129.80, 129.69, 128.12, 128.07, 127.52, 127.10, 126.82, 126.15, 126.11, 125.23, 123.45, 123.03, 122.88, 122.78, 122.62, 120.45, 119.83, 119.45, 119.19, 117.32, 115.02, 111.05, 107.86; HRMS DART (m/z) $[M+H]^+$: calcd. for $C_{38}H_{27}ON_2$: 527.2118; found: 527.2102.

Synthesis of *N^9-(dibenzo[b,d]thiophen-4-yl)-N^9,N^{10}-diphenylphenanthrene-9,10-diamine* (**I-**g)

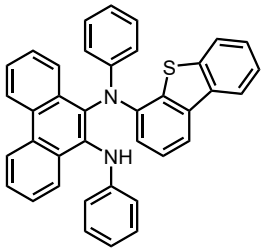

Purified by flash column chromatography on silica gel (PE/DCM = 10:1-3:1) to afford **I-**g as a white solid (1.30g, 88%). ^{1}H NMR (400 MHz, $CDCl_3$-*d*): δ 8.79 (d, *J* = 8.4 Hz, 2H), 8.14 – 8.03 (m, 2H), 7.98 (d, *J* = 8.3 Hz, 1H), 7.76 (m, 1H), 7.73 – 7.41 (m, 7H), 7.26 – 7.07 (m, 4H), 6.96 (t, *J* = 7.3 Hz, 2H), 6.85 (d, *J* = 8.2 Hz, 1H), 6.70 (t, *J* = 7.6 Hz, 2H), 6.53 (t, *J* = 7.3 Hz, 1H), 6.19 – 6.10 (m, 2H); ^{13}C NMR (101 MHz, $CDCl_3$-*d*): δ 145.10, 145.08, 140.30, 139.61, 137.60, 136.13, 135.72, 133.85, 132.99, 131.27, 130.52, 130.26, 129.67, 129.36, 128.10, 127.48, 127.04, 126.77, 126.21, 126.11, 125.71, 125.07, 124.39, 122.93, 122.85, 122.61, 122.59, 121.70, 121.41, 119.74, 119.11, 117.14, 115.07; HRMS DART (m/z) $[M+H]^+$: calcd. for $C_{38}H_{27}N_2S$: 543.1889; found: 543.1874.

Condition 2

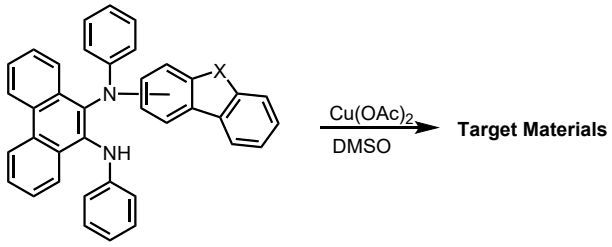

I

In a 10 mL round-bottom flask with a stir bar, **I-**x (1.0 equiv) and $Cu(OAc)_2$ (2.0 equiv) was added and dissolved in DMSO (using $CaCl_2$ drying tube as a desiccator) under air. The mixture was subsequently heated to 120 °C and monitored by TLC until **I-**x was completely consumed. After cooling to room temperature, the mixture was quenched with water and filtered. The filtrate was diluted and extracted with EtOAc (25ml), washed with brine for three times and the organic extracts were then combined and concentrated in vacuo. Purification by column chromatography yielded the desired

product.

Synthesis of *9,16,17-triphenyl-16,17-dihydro-9H-dibenzo[a,c]indolo[2,3-h]phenazine* **(DPAC-*w*-3,4-phCz)**

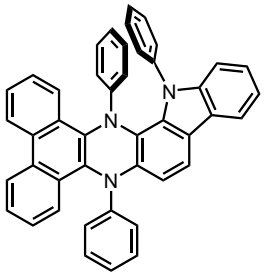

Condition 2 was followed on 600 mg (1 mmol) scale with a reaction time of 10 hours and purification by flash column chromatography on silica gel (PE/DCM = 4:1 to 2:1), **DPAC-*w*-3, 4-phCz** was obtained as a white solid (348 mg, 58%). ^{1}H NMR (600 MHz, DMSO-d_6): δ 8.88 (m, 2H), 8.32 (m, 2H), 8.00 (m, 1H), 7.91 (d, J = 8.3 Hz, 1H), 7.72 – 7.62 (m, 3H), 7.58 (m, 1H), 7.55 – 7.29 (m, 6H), 7.15 – 6.96 (m, 5H), 6.94 – 6.85 (m, 3H), 6.82 (m, 1H), 6.69 – 6.64 (m, 1H), 6.44 – 6.33 (m, 3H); ^{13}C NMR (151 MHz, $CDCl_3$-*d*): δ 149.17, 147.64, 145.60, 144.51, 139.92, 139.12, 138.10, 130.09, 129.93, 129.64, 129.49, 129.28, 128.55, 128.11, 128.03, 126.85, 126.64, 126.58, 126.29, 125.88, 125.67, 124.83, 123.41, 122.98, 122.89, 122.38, 121.43, 120.43, 119.90, 119.80, 118.93, 118.17, 117.78, 115.60, 110.66; HRMS DART (m/z) $[M+H]^+$: calcd. for $C_{44}H_{30}N_3$: 600.2434; found: 600.2412.

Synthesis of *9,17-diphenyl-9,17-dihydrodibenzo[a,c]benzo[4,5]thieno[2,3-h]phenazine* **(DPAC-*w*-3,4-DBT)**

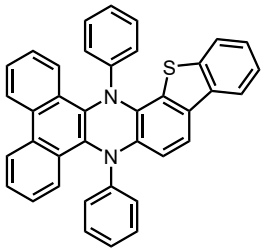

Condition 2 was followed on 540 mg (1 mmol) scale with a reaction time of 10 hours and purification by flash column chromatography on silica gel (PE/DCM = 4:1 to 2:1), **DPAC-*w*-3, 4-DBT** was obtained as a white solid (405 mg, 75%). ^{1}H NMR (600 MHz, DMSO-d_6): δ 9.01 – 8.96 (m, 2H), 8.48 – 8.42 (m, 2H), 8.30 (m, 1H), 8.19 (d, J = 8.4

Hz, 1H), 8.10 – 8.06 (m, 1H), 7.99 (m, 1H), 7.81 (m, 2H), 7.73 (m, 1H), 7.61 (m, 1H), 7.56 (m, 2H), 7.09 (m, 4H), 7.04 – 6.99 (m, 2H), 6.87 (m, 1H), 6.75 (t, *J* = 7.3 Hz, 1H), 6.65 – 6.59 (m, 2H); ^{13}C NMR (151 MHz, $CDCl_3$-*d*): δ 147.37, 147.14, 145.06, 139.71, 139.38, 139.29, 138.91, 138.42, 138.40, 135.57, 133.88, 130.35, 130.07, 129.56, 129.27, 128.73, 128.53, 127.44, 126.85, 126.70, 126.60, 124.74, 124.62, 124.60, 123.91, 123.06, 122.97, 122.86, 121.66, 121.64, 120.34, 118.90, 117.95, 115.42; HRMS DART (m/z) $[M+H]^+$: calcd. for $C_{38}H_{25}N_2S$: 541.1733; found: 541.1721.

Synthesis of *9-phenyl-14-(9-phenyl-9H-carbazol-4-yl)-9,14-dihydrodibenzo[a,c] phenazine* **(DPAC-*h*-1-phCz)**

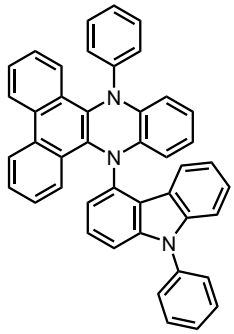

Condition 2 was followed on 600 mg (1 mmol) scale with a reaction time of 10 hours and purification by flash column chromatography on silica gel (PE/DCM = 4:1 to 2:1), **DPAC-*h*-1-phCz** was obtained as a white solid (430 mg, 72%). ^{1}H NMR (600 MHz, DMSO-d_6): δ 8.91 – 8.87 (m, 2H), 8.44 (d, *J* = 8.0 Hz, 1H), 8.21 – 8.19 (m, 1H), 8.09 – 8.07 (m, 1H), 7.79 (m, 1H), 7.77 – 7.66 (m, 6H), 7.61 – 7.56 (m, 2H), 7.55 – 7.50 (m, 2H), 7.36 (m, 1H), 7.32 (m, 1H), 7.29 (d, *J* = 8.1 Hz, 1H), 7.25 (m, 1H), 7.20 (m, 2H), 7.09 – 7.04 (m, 3H), 6.94 (m, 3H), 6.69 (d, *J* = 7.6 Hz, 1H); ^{13}C NMR (151 MHz, DMSO-d_6): δ 150.44, 146.01, 142.63, 142.30, 141.18, 138.91, 138.37, 136.84, 131.75, 130.71, 130.21, 129.49, 129.35, 129.06, 128.60, 128.21, 128.07, 128.01, 127.53, 127.45, 127.37, 127.14, 126.86, 126.71, 126.52, 124.20, 124.04, 123.87, 123.80, 123.36, 121.96, 121.85, 121.43, 121.25, 120.39, 120.20, 116.40, 110.61, 109.60; HRMS DART (m/z) $[M+H]^+$: calcd. for $C_{44}H_{30}N_3$: 600.2434; found: 600.2412.

Synthesis of *9-(dibenzo[b,d]thiophen-1-yl)-14-phenyl-9,14-dihydrodibenzo[a,c]phen-azine* **(DPAC-*h*-1-DBT)**

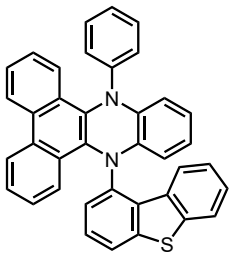

Condition 2 was followed on 540 mg (1 mmol) scale with a reaction time of 10 hours and purification by flash column chromatography on silica gel (PE/DCM = 4:1 to 2:1), **DPAC-*h*-1-DBT** was obtained as a white solid (442 mg, 82%). ^{1}H NMR (600 MHz, DMSO-d_6): δ 8.91 – 8.85 (m, 2H), 8.57 (d, J = 8.2 Hz, 1H), 8.24 – 8.17 (m, 2H), 8.08 (m, 1H), 7.79 (m, 1H), 7.69 (m, 3H), 7.59 (m, 1H), 7.49 (m, 1H), 7.32 (m, 1H), 7.28 – 7.18 (m, 4H), 7.00 (m, 2H), 6.97 – 6.88 (m, 5H); ^{13}C NMR (151 MHz, DMSO-d_6): δ 150.70, 144.50, 143.48, 141.46, 139.86, 137.85, 137.50, 134.34, 133.86, 130.29, 130.13, 129.59, 129.56, 129.42, 129.00, 128.27, 128.25, 128.11, 128.04, 128.01, 127.32, 126.86, 126.83, 126.78, 126.64, 126.53, 126.45, 125.83, 125.46, 124.19, 124.14, 123.74, 123.73, 123.70, 123.47, 123.23, 121.59, 119.43, 116.55; HRMS DART (m/z) $[M+H]^+$: calcd. for $C_{38}H_{25}N_2S$: 541.1733; found: 541.1719.

Synthesis of *9-(9,9-dimethyl-9H-fluoren-4-yl)-14-phenyl-9,14-dihydrodibenzo[a,c] phenazine* **(DPAC-*h*-1-DMI)**

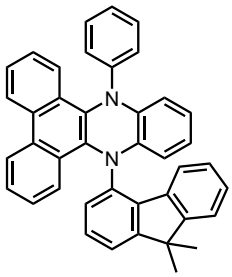

Condition 2 was followed on 550 mg (1 mmol) scale with a reaction time of 10 hours and purification by flash column chromatography on silica gel (PE/DCM = 4:1 to 2:1), **DPAC-*h*-1-DMI** was obtained as a white solid (485 mg, 88%). ^{1}H NMR (600 MHz, DMSO-d_6): δ 8.90 – 8.84 (m, 2H), 8.22 – 8.17 (m, 1H), 7.98 (d, J = 7.8 Hz, 1H), 7.82 (m, 1H), 7.77 (d, J = 7.8 Hz, 1H), 7.72 (d, J = 7.6 Hz, 1H), 7.67 (m, 2H), 7.57 (d, J = 7.4 Hz, 1H), 7.50 (m, 1H), 7.42 (m, 1H), 7.25 – 7.15 (m, 4H), 7.11 – 7.02 (m, 4H), 6.93

(t, J = 7.2 Hz, 1H), 6.90 – 6.85 (m, 2H), 6.73 (d, J = 7.8 Hz, 1H), 1.58 (d, J = 3.6 Hz, 6H); ^{13}C NMR (151 MHz, DMSO-d_6): δ 156.44, 154.57, 150.72, 144.90, 141.69, 137.92, 137.77, 137.65, 137.54, 130.31, 130.27, 129.46, 129.44, 129.20, 128.93, 128.56, 128.04, 128.02, 127.71, 127.65, 127.54, 126.75, 126.72, 126.52, 126.48, 124.71, 124.06, 123.86, 123.72, 123.68, 123.63, 123.33, 122.77, 121.45, 119.73, 116.43, 47.22, 40.36, 40.22, 40.08, 39.93, 39.79, 39.65, 39.51, 27.52, 27.31; HRMS DART (m/z) $[M+H]^+$: calcd. for $C_{41}H_{31}N_2$: 551.2482; found: 551.2466.

Synthesis of *9-(dibenzo[b,d]furan-1-yl)-14-phenyl-9,14-dihydrodibenzo[a,c]phenazine* **(DPAC-*h*-1-DBF)**

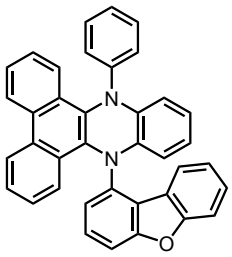

Condition 2 was followed on 525 mg (1 mmol) scale with a reaction time of 10 hours and purification by flash column chromatography on silica gel (PE/DCM = 4:1 to 2:1), **DPAC-*h*-1-DBF** was obtained as a white solid (420 mg, 80%). ^{1}H NMR (600 MHz, DMSO-d_6): δ 8.92 – 8.86 (m, 2H), 8.29 (m, 1H), 8.20 – 8.16 (m, 1H), 7.95 – 7.86 (m, 2H), 7.82 (m, 1H), 7.75 – 7.65 (m, 4H), 7.54 – 7.47 (m, 2H), 7.31 – 7.24 (m, 2H), 7.24 – 7.17 (m, 3H), 7.09 (m, 2H), 7.00 – 6.93 (m, 3H), 6.81 (d, J = 7.9 Hz, 1H); ^{13}C NMR (151 MHz, DMSO-d_6): δ ^{13}C NMR (151 MHz, DMSO) δ 156.92, 156.22, 150.19, 145.85, 142.66, 139.17, 137.96, 132.30, 130.24, 129.55, 129.20, 129.13, 128.95, 128.93, 128.09, 128.06, 128.02, 127.20, 126.93, 126.88, 126.69, 124.43, 124.40, 124.15, 123.96, 123.83, 123.69, 123.54, 123.11, 123.07, 122.94, 121.63, 120.23, 116.63, 112.66, 111.65; HRMS DART (m/z) $[M+H]^+$: calcd. for $C_{38}H_{25}ON_2$: 525.1961; found: 525.1944.

Synthesis of *9-(dibenzo[b,d]thiophen-4-yl)-14-phenyl-9,14-dihydrodibenzo[a,c]phenazine* (**DPAC-*h*-4-DBT**)

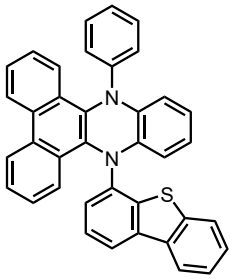

Condition 2 was followed on 540 mg (1 mmol) scale with a reaction time of 12 hours and purification by flash column chromatography on silica gel (PE/DCM = 3:1), **DPAC-*h*-4-DBT** was obtained as a white solid (421 mg, 78%). ^{1}H NMR (600 MHz, DMSO-d_6): δ 8.90 (t, J = 7.7 Hz, 2H), 8.37 – 8.32 (m, 1H), 8.24 (d, J = 7.7 Hz, 1H), 8.15 (m, 1H), 8.14 – 8.08 (m, 2H), 7.95 – 7.90 (m, 1H), 7.81 (m, 1H), 7.72 (m, 2H), 7.57 (m, 1H), 7.54 – 7.48 (m, 3H), 7.38 – 7.28 (m, 4H), 7.19 – 7.15 (m, 2H), 6.99 (d, J = 8.3 Hz, 2H), 6.90 (t, J = 7.3 Hz, 1H); ^{13}C NMR (151 MHz, DMSO-d_6): δ 148.18, 145.94, 142.75, 140.08, 138.58, 138.01, 137.93, 136.91, 135.30, 133.72, 129.96, 129.33, 129.03, 128.49, 128.10, 128.05, 127.90, 127.36, 127.16, 127.10, 126.63, 126.50, 125.68, 125.46, 125.30, 124.38, 124.15, 123.97, 123.26, 122.96, 122.84, 122.48, 121.10, 120.77, 115.87; HRMS DART (m/z) $[M+H]^+$: calcd. for $C_{38}H_{25}N_2S$: 541.1733; found: 541.1721.

Condition 3

Synthesis of *9,17-diphenyl-9,17-dihydrodibenzo[a,c]benzo[4,5]thieno[2,3-h]phenazine 16,16-dioxide* **(DPAC-*w*-3,4-DBTS)**

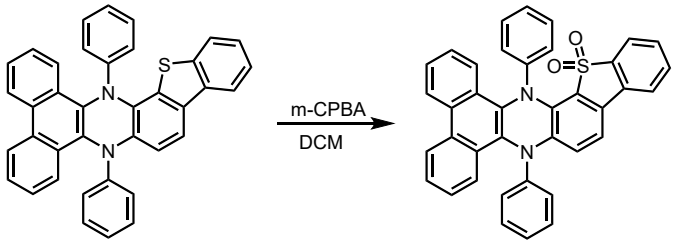

DPAC-*w*-3,4-DBT **DPAC-*w*-3,4-DBTS**

In a 10 mL round-bottom flask with a stir bar, **DPAC-*w*-3,4-DBT** (1.0 equiv) and m-CPBA (3.0 equiv) was added and dissolved in DCM under air. The mixture was stirred at r.t. for 1h, and then combined and concentrated in vacuo. Purification by column

chromatography yielded the desired product.

Condition 3 was followed on 270 mg (0.5 mmol) scale with a reaction time of 1 hour and purification by flash column chromatography on silica gel (PE/DCM = 1:1), **DPAC-*w*-3, 4-DBTS** was obtained as a white solid (245 mg, 85%). ^{1}H NMR (600 MHz, DMSO-d_6): δ 8.98 (d, J = 8.3 Hz, 2H), 8.45 (m, 2H), 8.28 (m, 2H), 7.96 (d, J = 7.7 Hz, 1H), 7.90 – 7.86 (m, 1H), 7.86 – 7.78 (m, 3H), 7.72 (m, 1H), 7.66 (t, J = 7.6 Hz, 1H), 7.56 (t, J = 7.6 Hz, 1H), 7.11 (m, 4H), 7.04 – 6.94 (m, 3H), 6.78 (t, J = 7.3 Hz, 1H), 6.60 (d, J = 8.3 Hz, 2H); ^{13}C NMR (151 MHz, $CDCl_3$-*d*): δ 149.80, 149.21, 146.17, 140.17, 138.94, 138.32, 138.01, 134.52, 133.76, 130.94, 130.63, 130.53, 130.35, 129.93, 129.63, 129.09, 128.60, 128.31, 128.08, 127.09, 126.80, 126.69, 125.15, 124.37, 123.34, 123.29, 122.62, 122.19, 121.33, 121.18, 120.18, 119.26, 116.11; HRMS DART (m/z) $[M+H]^+$: calcd. for $C_{38}H_{25}O_2N_2S$: 573.1631; found: 573.1611.

3. X-ray crystal structures

Table S1. CCDC.NO, crystal data and structure refinements.

	DPAC-*h*-1-DMI	**DPAC-*h*-1-DBF**	**DPAC-*h*-1-phCz**	**DPAC-*w*-3, 4-phCz**
CCDC	2448858	2448869	2448863	2448864
Empirical formula	$C_{41}H_{30}N_2$	$C_{38}H_{24}N_2O$	$C_{44}H_{29}N_3$	$C_{44}H_{29}N_3$
Formula wt	550.67	524.59	599.70	599.70
T, k	213(2)	213	213(2)	213(2)
Crystal system	Triclinic	Triclinic	Monoclinic	Monoclinic
Space group	P -1	P -1	P 21/n	C 2/c
a, Å	8.3035(4)	11.4470(5)	11.7112(6)	26.2731(9)
b, Å	12.6508(7)	11.8077(5)	22.4077(10)	14.8626(5)
c, Å	15.4990(7)	20.7420(9)	11.9472(5)	16.0088(5)
α, deg	113.3470(10)	86.1150(10)°	90°	90°
β, deg	96.581(2)°	80.2380(10)°	95.491(2)°	95.5630(10)°
γ, deg	94.812(2)°	89.4690(10)°	90°	90°
V, Å^3	1469.95(13)	2756.6(2)	3120.8(2)	6221.8(4)
Z	2	4	4	8
Density, Mg/m^3	1.244	1.264	1.276	1.280
μ (Mo Kα), mm^{-1}	0.072	0.076	0.075	0.075
θ range, deg	2.711°-25.998°	2.728°-27.531°	1.969°-26.000°	2.741°-25.999°
No. of reflections collected	26379	59953	32737	32036
No. of independent reflections	5753	12609	6129	6108
R (int)	0.0446	0.0471	0.0786	0.0761
GOF	1.030	1.204	1.034	1.073
R_1 [$I > 2\sigma(I)$]	0.0445	0.0548	0.0520	0.0672
wR_2 [$I > 2\sigma(I)$]	0.1014	0.1644	0.1068	0.1285
R_1 (all data)	0.0585	0.0777	0.0942	0.1190
wR_2 (all data)	0.1109	0.1799	0.1263	0.1529
	DPAC-*h*-	**DPAC-*h*-**	**DPAC-*w*-**	**DPAC-*w*-**

	1-DBT	**4-DBT**	**3, 4-DBT**	**3, 4-DBTS**
CCDC	2448865	2448866	2448870	2448873
empirical formula	$C_{38}H_{24}N_2S$	$C_{38}H_{24}N_2S.CH_2Cl_2$	$C_{38}H_{24}N_2S$	$C_{38}H_{24}N_2O_2S$
formula wt	540.65	625.58	540.65	572.65
T, k	213(2)	213(2)	213(2)	170
crystal system	Orthorhombic	Triclinic	Monoclinic	Triclinic
Space group	I b a 2	P -1	P 21/n	P -1
a, Å	15.0172(5)	11.1081(4)	15.1168(7)	8.7316(8)
b, Å	45.2600(17)	12.0105(4)	34.5885(15)	10.9941(10)
c, Å	7.7848(2)	12.3126(4)	10.4028(4)	15.4026(15)
α, deg	90°	72.6750(10)°	90°	94.571(4)°
β, deg	90°	73.2960(10)°	97.5590(10)°	104.728(4)°
γ, deg	90°	85.6620(10)°	90°	102.244(4)°
V, Å^3	5291.2(3)	1501.88(9)	5392.0(4)	1383.4(2)
Z	8	2	8	2
density, g/cm^3	1.357	1.383	1.332	1.375
μ (Mo Kα), mm^{-1}	0.155	0.319	0.152	0.880
θ range, deg	2.627°-25.987°	1.914°-26.000°	2.650°-25.999°	3.615°-55.479°
No. of reflections collected	46503	41505	50531	5170
No. of independent reflections	5197	5897	10579	5170
R (int)	0.0808	0.0603	0.0939	
GOF	1.095	1.035	1.057	1.213
R_1 [$I > 2\sigma(I)$]	0.0431	0.0626	0.0695	0.0981
wR_2 [$I > 2\sigma(I)$]	0.0783	0.1573	0.1348	0.2996
R_1 (all data)	0.0614	0.0836	0.1322	0.1036
wR_2 (all data)	0.0861	0.1742	0.1627	0.3056

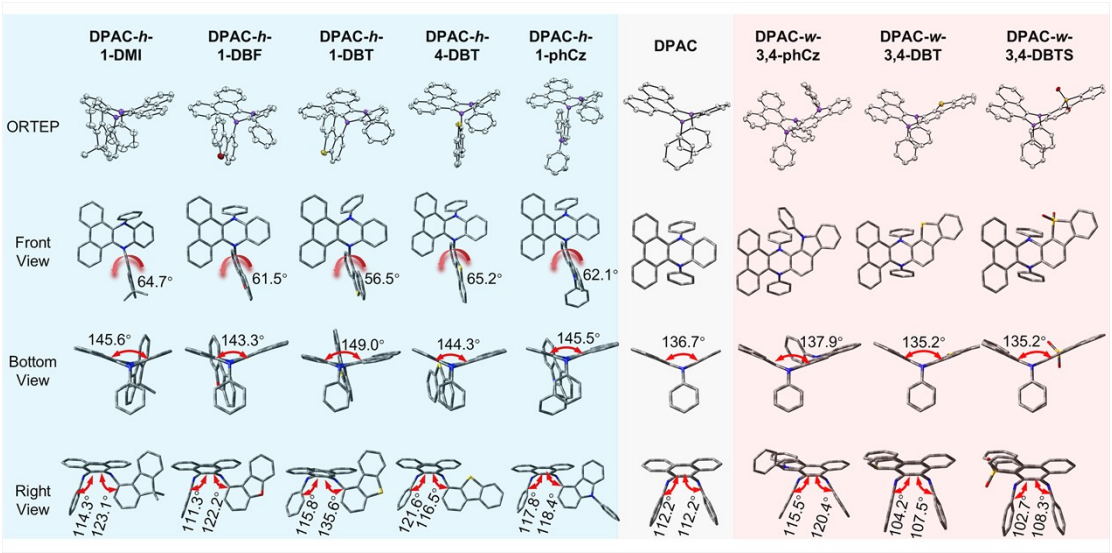

Figure S1. Single-crystal structures of **DPAC** derivatives and three perspectives with key angles. Hydrogens have been omitted for clarity. Note that the background color indicates different series of molecules, i.e., blue, **DPAC-*h*** series; gray, **DPAC;** red, **DPAC-*w*** series.

Table S2. Calculated f_A^- value for **I**.

	I-a			**I**-d		**I**-e		**I**-f	
reactive site	C1	C2	C3	C1	C2	C1	C2	C1	C2
f_A^-	0.0234	0.0193	0.0302	0.0211	0.0135	0.0242	0.0069	0.0242	0.0152

4. Photophysical properties

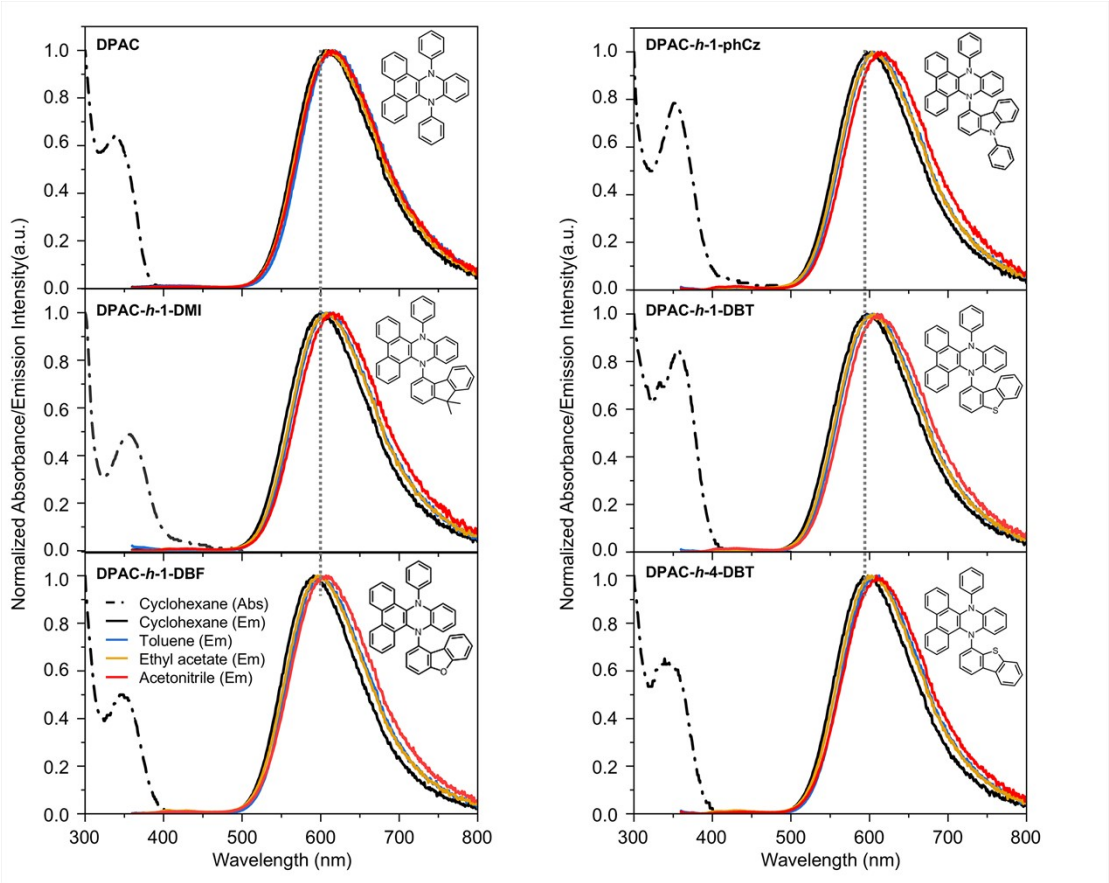

Figure S2. Normalized absorption and emission spectra of **DPAC** and **DPAC-*h*** derivatives in various solvents from nonpolar cyclohexene to polar acetonitrile.

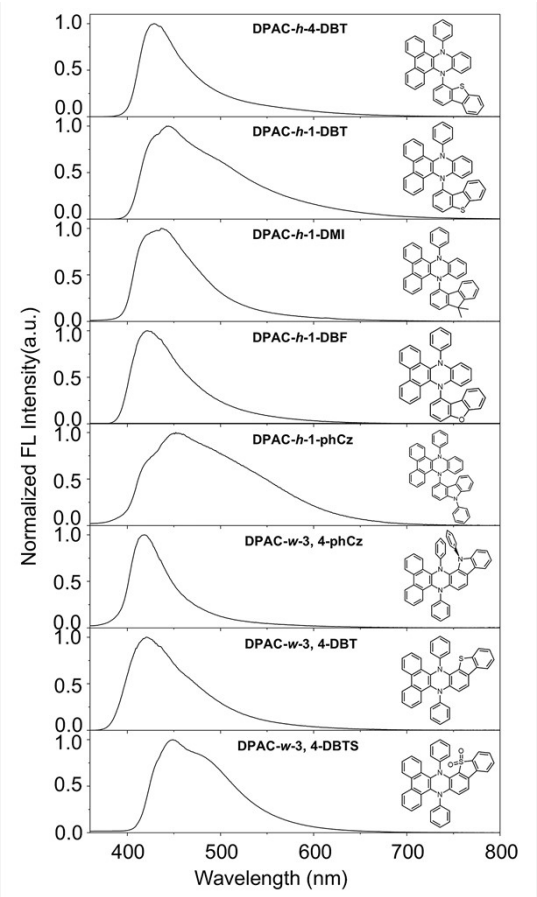

Figure S3. Normalized solid powder emission spectra of **DPAC** derivatives at room temperature.

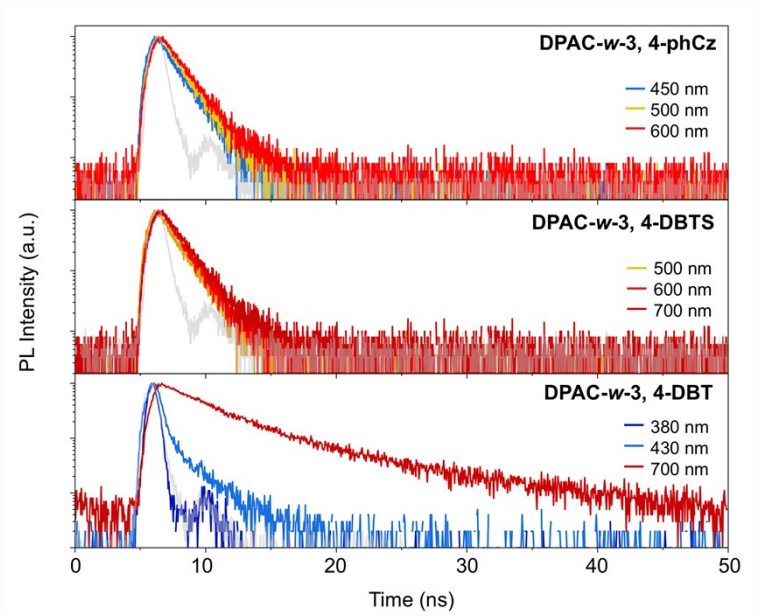

Figure S4. Fluorescence decay profiles of **DPAC-*w*** derivatives at various wavelength in cyclohexane.

Table S3. Fitting results of TCSPC spectroscopic measurements for **DPAC-*w*-3, 4-DBT**, **DPAC-*w*-3, 4-DBTS** and **DPAC-*w*-3, 4-phCz** in cyclohexane.

Counpond	**DPAC-*w*-3, 4-phCz**			**DPAC-*w*-3, 4-DBTS**			**DPAC-*w*-3, 4-DBT**		
λ_{probe} (nm)	450	500	600	500	600	700	380	430	700
τ1 (ns)	1.92	2.02	2.05	1.28	1.35	1.39		0.45	4.73
τ2 (ns)								2.45	

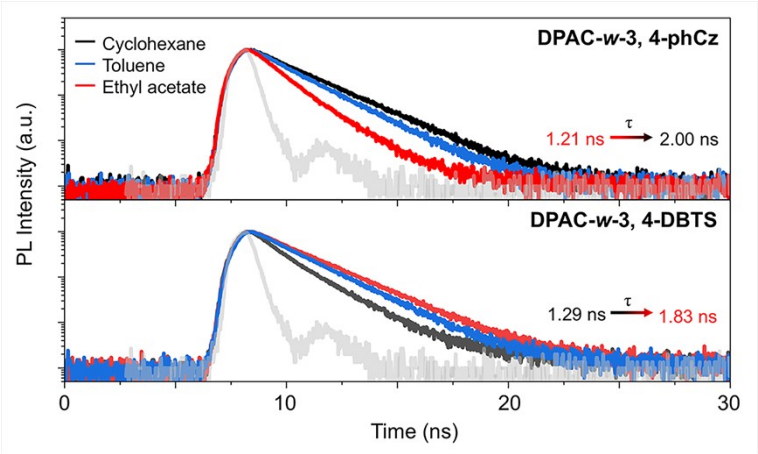

Figure S5. Fluorescence decay profiles of **DPAC-*w*-3,4-phCz** and **DPAC-*w*-3,4-DBTS** in various solutions at respective maximum emission wavelength.

Table S4. Fitting results of TCSPC spectroscopic measurements for **DPAC-*w*-3, 4-phCz** and **DPAC-*w*-3, 4-DBTS** in various solutions at respective maximum emission wavelength.

Compound	**DPAC-*w*-3, 4-phCz**			**DPAC-*w*-3, 4-DBTS**		
Solvent	cyclohexane	toluene	ethyl acetate	cyclohexane	toluene	ethyl acetate
Wavelength (nm)	495	495	495	540	557	580
Lifetime (τ_1, ns)	2.00	1.73	1.21	1.29	1.61	1.83

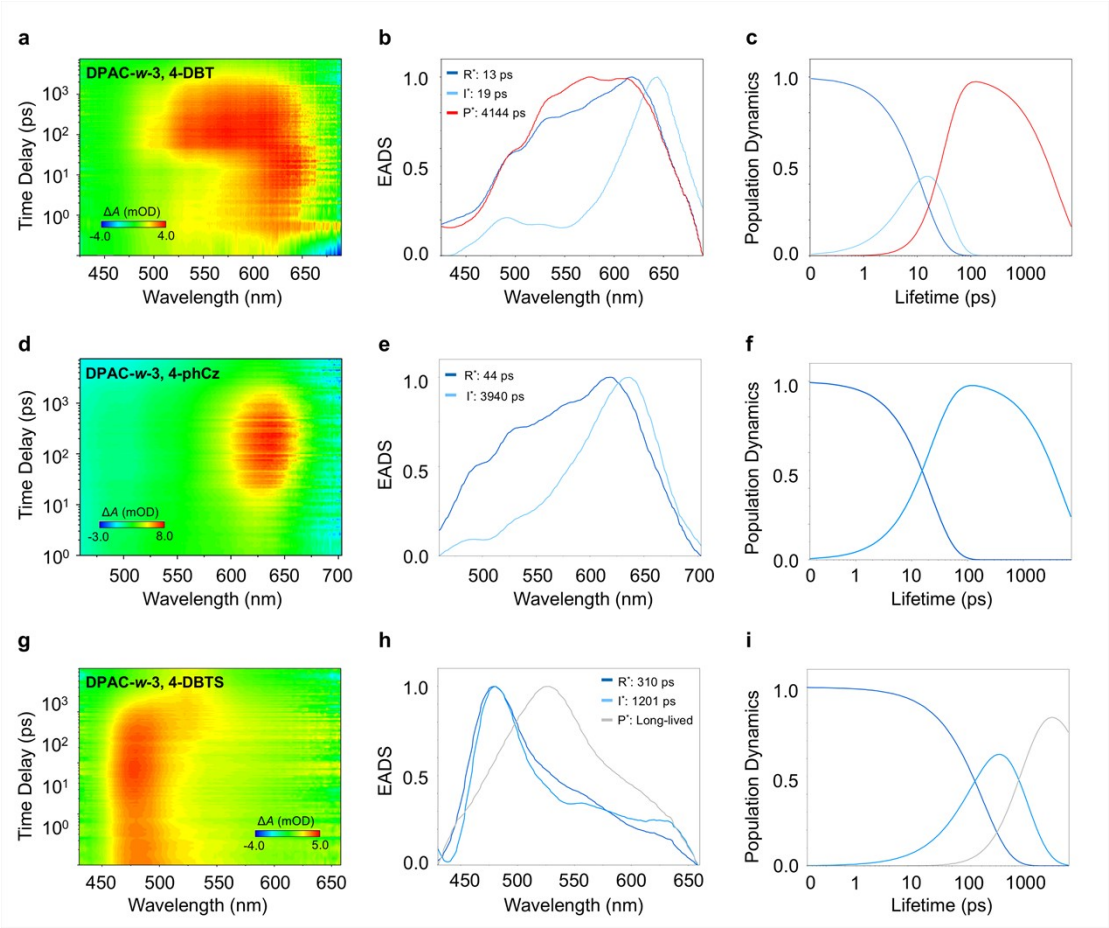

Figure S6. Pseudocolor TA plot, corresponding evolution-associated difference spectra (EADS) from global analysis and population dynamics of transient species of **DPAC**-based derivatives.

5. Theoretical calculation

5.1 Electronic excitation

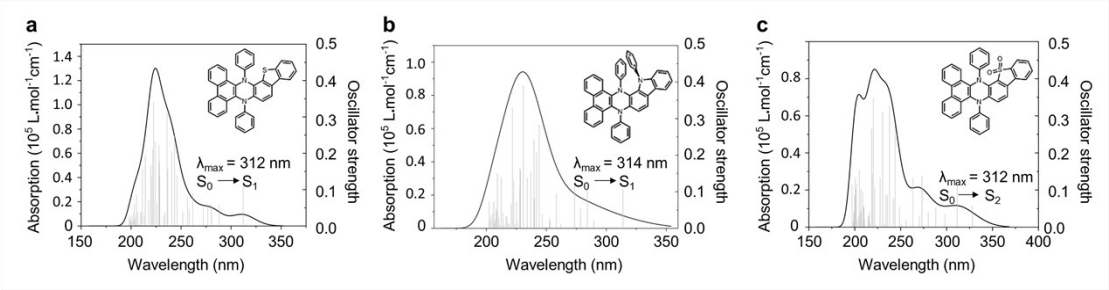

Figure S7. Simulated UV-Vis absorption spectrum (curve) and oscillator strength (black spikes) of (a) **DPAC-*w*-3,4-DBT**, (b) **DPAC-*w*-3,4-phCz** and (c) **DPAC-*w*-3,4-DBTS**.

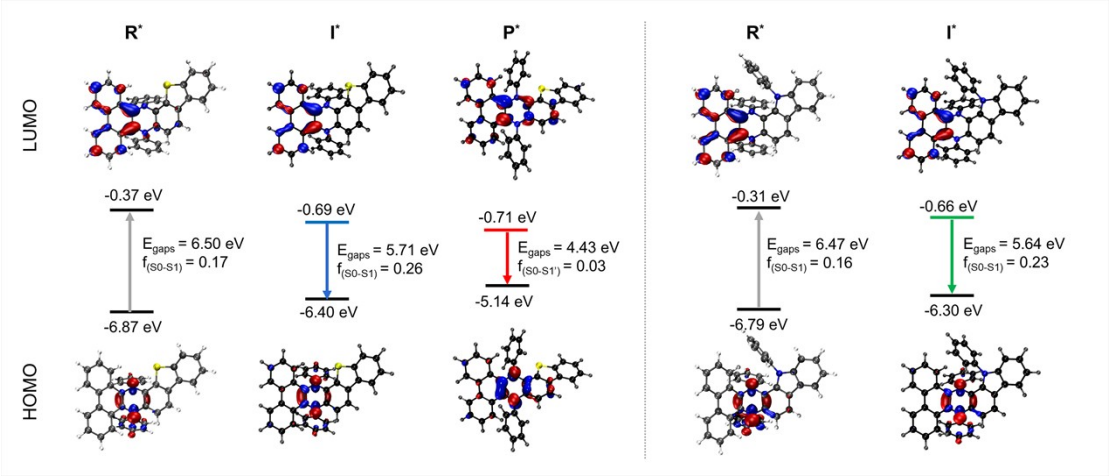

Figure S8. Electron density distributions of HOMO and LUMO for excited state of (a) **DPAC-*w*-3,4-DBT** and (b) **DPAC-*w*-3,4-phCz**.

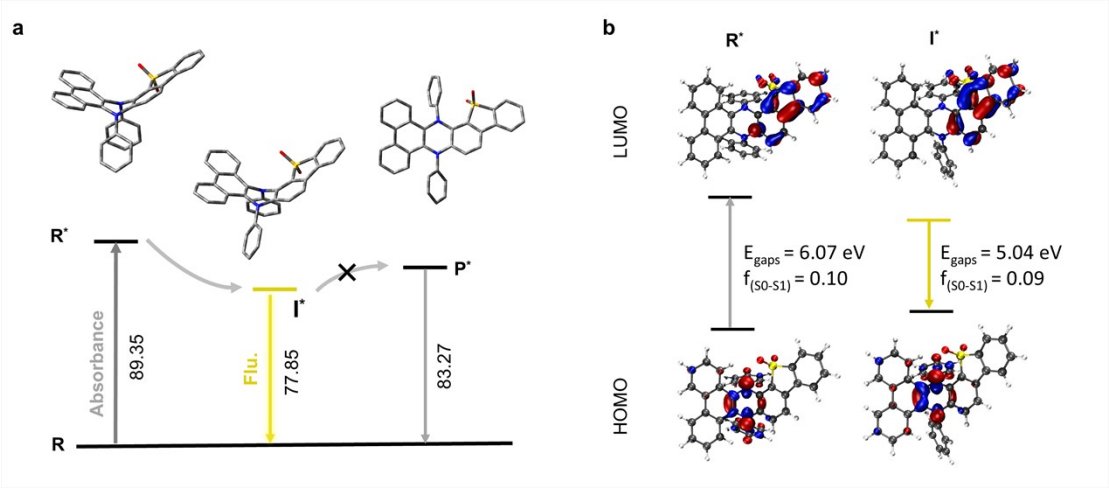

Figure S9. (a) Optimized excited-state geometries and relative energy levels (kcal mol^{-1}) and (b) Electron density distributions of HOMO and LUMO for excited state of **DPAC-*w*-3,4-DBTS.**

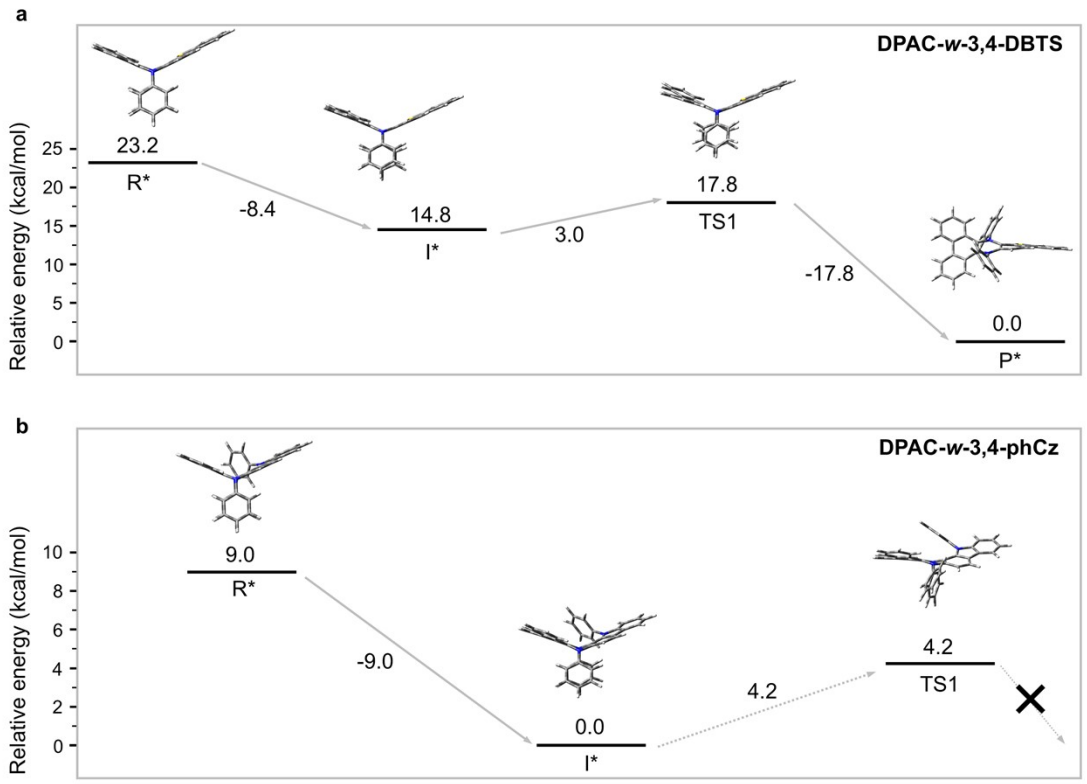

Figure S10. Optimized excited-state geometries and relative energy levels (kcal mol^{-1}) of **DPAC-*w*-3,4-DBT** and **DPAC-*w*-3,4-phCz**.

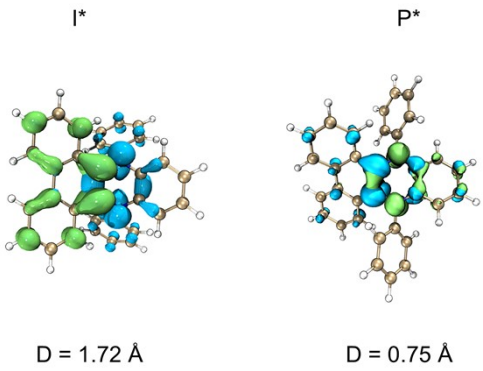

Figure S11. The electron and hole iso-surfaces of **DPAC** (hole (green)-ele (blue)). D-index was used to show the distance between the center of electrons and holes.

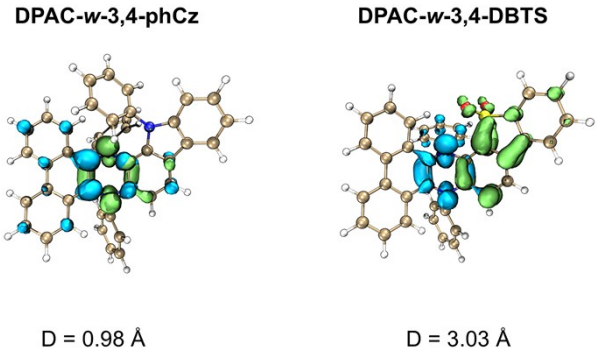

Figure S12. The electron and hole iso-surfaces for **DPAC-w-3,4-phCz** and **DPAC-w-3,4-DBTS** of I* state (hole (green)-ele (blue)). D-index was used to show the distance between the center of electrons and holes.

6. Thermal and electrochemical properties

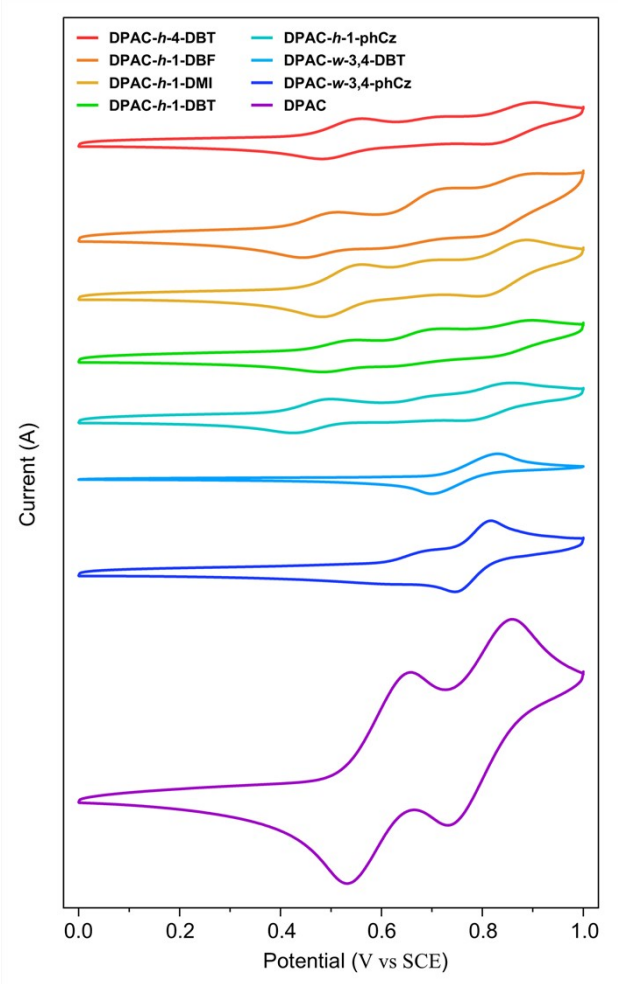

Figure S13. CV characteristics of **DPAC** derivatives.

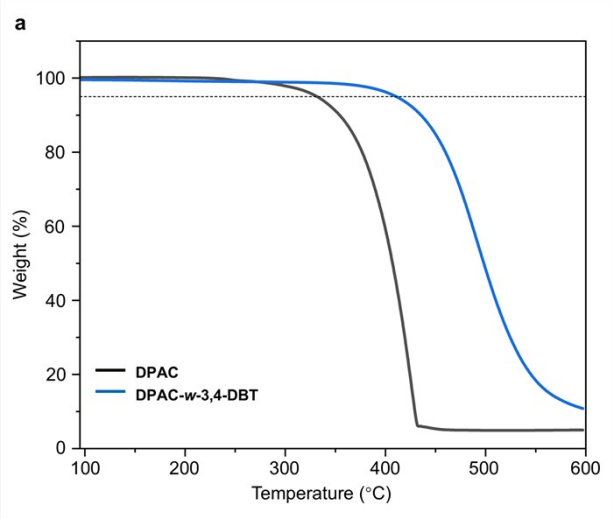

Figure S14. TGA curves of **DPAC** and **DPAC-*w*-3, 4-DBT**.

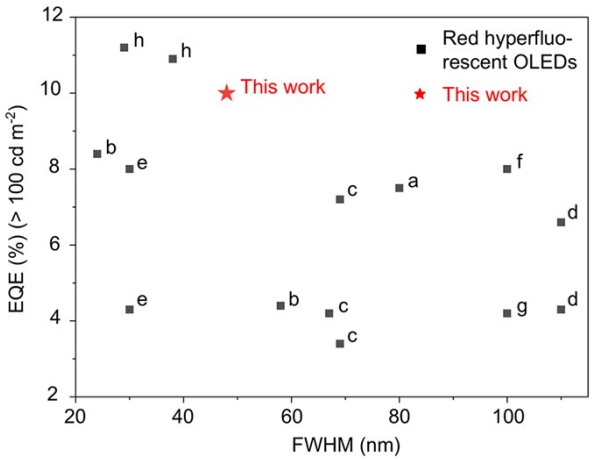

Figure S15. EQEs (%) (>100 cd m^{-2}) of hyperfluorescent OLEDs versus electroluminescent FWHM (nm). Black square represents a series of red hyperfluorescent OLEDs, and the red star represents this work. Reference according to number label.[9]

7. References

[1] E. Runge and E. K. Gross, Density-Functional Theory for Time Dependent Systems, *Phys. Rev. Lett.*, 1984, **52**, 997-1000.

[2] R. E. Stratmann, G. E. Scuseria and M.-J. Frisch, An Efficient Implementation of Time-dependent Density-functional Theory for the Calculation of Excitation Energies of Large Molecules, *J. Chem. Phys.*, 1998, **109**, 8218-8224.

[3] R. Krishnan, J. S. Binkley, R. Seeger and J. A. Pople, Self-consistent Molecular Orbital Methods. XX. A Basis Set for Correlated Wave Functions, *J. Chem. Phys.*, 1980, **72**, 650-654.

[4] T. Yanai, D. P. Tew and N. C. Handy, A New Hybrid Exchange-correlation Functional Using the Coulomb-attenuating Method (CAM-B3LYP), *Chem. Phys. Lett.*, 2004, **393**, 51–57.

[5] S. Grimme, J. Antony, S. Ehrlich and H. Krieg, A Consistent and Accurate Ab Initio Parametrization of Density Functional Dispersion Correction (DFT-D) for the 94 Elements H-Pu, *J. Chem. Phys.*, 2010, **132**, 154104-154501.

[6] Gaussian 16, Revision C.01. M. J. Frisch, G. W. Trucks, H. B. Schlegel, G. E. Scuseria, M. A. Robb, J. R. Cheeseman, G. Scalmani, V. Barone, G. A. Petersson, H. Nakatsuji, X. Li, M. Caricato, A. V. Marenich, J. Bloino, B. G. Janesko, R. Gomperts, B. Mennucci, H. P. Hratchian, J. V. Ortiz, A. F. Izmaylov, J. L. Sonnenberg, D. Williams-Young, F. Ding, F. Lipparini, F. Egidi, J. Goings, B. Peng, A. Petrone, T. Henderson, D. Ranasinghe, V. G. Zakrzewski, J. Gao, N. Rega, G. Zheng, W. Liang, M. Hada, M. Ehara, K. Toyota, R. Fukuda, J. Hasegawa, M. Ishida, T. Nakajima, Y. Honda, O. Kitao, H. Nakai, T. Vreven, K. Throssell, J. A. Jr. Montgomery, J. E. Peralta, F. Ogliaro, M. J. Bearpark, J. J. Heyd, E. N. Brothers, K. N. Kudin, V. N. Staroverov, T. A. Keith, R. Kobayashi, J. Normand, K. Raghavachari, A. P. Rendell, J. C. Burant, S. S. Iyengar, J. Tomasi, M. Cossi, J. M. Millam, M. Klene, C. Adamo, R. Cammi, J. W. Ochterski, R. L. Martin, K. Morokuma, O. Farkas, J. B. Foresman and D. J. Fox, Gaussian, Inc. Wallingford CT, 2016.

[7] T. Lu and F. Chen, Multiwfn: A Multifunctional Wavefunction Analyzer, *J.*

Comput. Chem., 2012, **33**, 580-592.

[8] W. Humphrey, A. Dalke and K. Schulten, VMD: Visual Molecular Dynamics, *J. Mol. Graph.*, 1996, **14**, 33-38.

[9] (a) Q. Wang, L. Chen, Q. Yang, Y. Xu, H. Wang and Z. Xie, Efficient Solution-Processed Red Fluorescent OLEDs Using Diluted Exciplex Host to Reduce Non-Radiative Loss of Triplet Excitons, *Adv. Mater. Interfaces,* 2022, **9**, 2200830; (b) N. R. Wallwork, M. Mamada, A. Shukla, S. K. M. McGregor, C. Adachi, E. B. Namdas and S.-C. Lo, High-performance solution-processed red hyperfluorescent OLEDs based on cibalackrot, *J. Mater. Chem. C.*, 2022,**10**, 4767-4774; (c) S. Shen, Z. Pang, X. Xie, X. Lv, Q. Zhang, Q. Zhang and Y. Wang, DIPz-TPTRZ Exciplex Films: Dual-Role Emitters and Hosts for Stable OLEDs with High-Efficiency and Reduced Efficiency Roll-Off, *ACS Appl. Mater. Interfaces,* 2025, **17**, 14312-14321; (d) C.-Y. Huang, S.-Y. Ho, C.-H. Lai, C.-L. Ko, Y.-C. Wei, J.-A. Lin, D.-G. Chen, T.-Y. Ko, K.-T. Wong, Z. Zhang, W.-Y. Hung and P.-T. Chou, Insights into energy transfer pathways between the exciplex host and fluorescent guest: attaining highly efficient 710 nm electroluminescence, *J. Mater. Chem. C.,* 2020, **8**, 5704-5714; (e) D. Chen, X. Cai, X.-L. Li, Z. He, C. Cai, D. Chen, and S.-J. Su, Efficient solution-processed red all-fluorescent organic light-emitting diodes employing thermally activated delayed fluorescence materials as assistant hosts: molecular design strategy and exciton dynamic analysis, *J. Mater. Chem. C.,* 2017, **5**, 5223-5231; (f) L.-M. Chen, I.-H. Lin, Y.-C. You, W.-C. Wei, M.-J. Tsai, W.-Y. Hung and K.-T. Wong, Substitution effect on carbazole-centered donors for tuning exciplex systems as cohost for highly efficient yellow and red OLEDs, *Mater. Chem. Front.,* 2021, **5**, 5044-5054; (g) H.-Z. Li, F.-M. Xie, P. Wu, K. Zhang, X. Zhao, Y.-Q. Li and J.-X. Tang, Asymmetric donor–acceptor–host red thermally activated delayed fluorescent emitter for high-efficiency organic light emitting diodes, *J. Mater. Chem. C.,* 2023, **11**, 9348-9354; (h) X. Nie, Z. Li, S. Chen, Z. Chen, Y. Fu, Z. Yang, G. Yang, Y. Ren, X. Cheng, Y. Zeng, Y. Tian, D. Liu, M. Li, J. Kido and S.-J. Su, Highly Horizontally Oriented BODIPY Emitters for Efficient BT. 2020 Red OLEDs via Low-Polarity Multi-Sensitization Strategy, *Adv.*

Funct. Mater., 2025, e29876.

8. HRMS, ^{1}H NMR and ^{13}C NMR spectrum

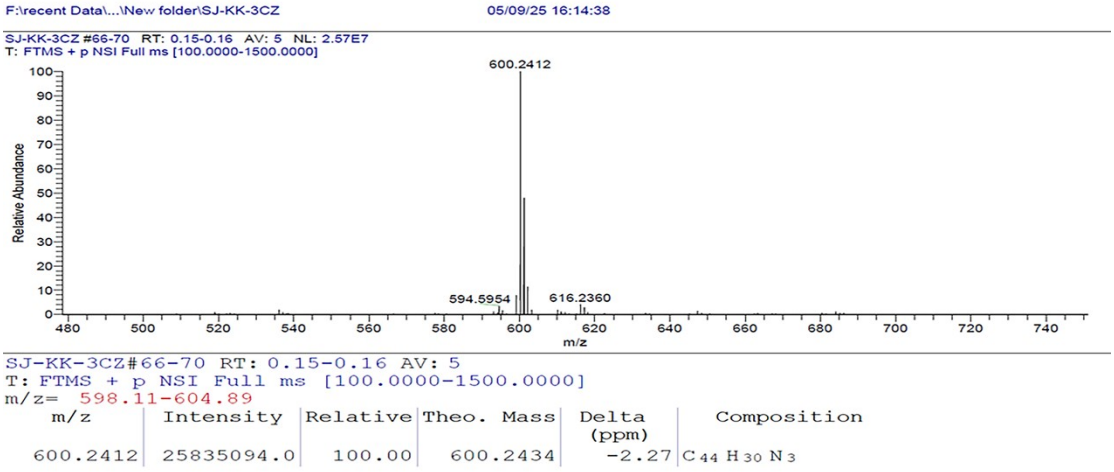

SJ-KK-3CZ#66-70 RT: 0.15-0.16 AV: 5
T: FTMS + p NSI Full ms [100.0000-1500.0000]
m/z= 598.11-604.89

m/z	Intensity	Relative	Theo. Mass	Delta (ppm)	Composition
600.2412	25835094.0	100.00	600.2434	-2.27	$C_{44}H_{30}N_3$

Figure S16. HRMS spectrum of **DPAC-*w*-3,4-phCz**.

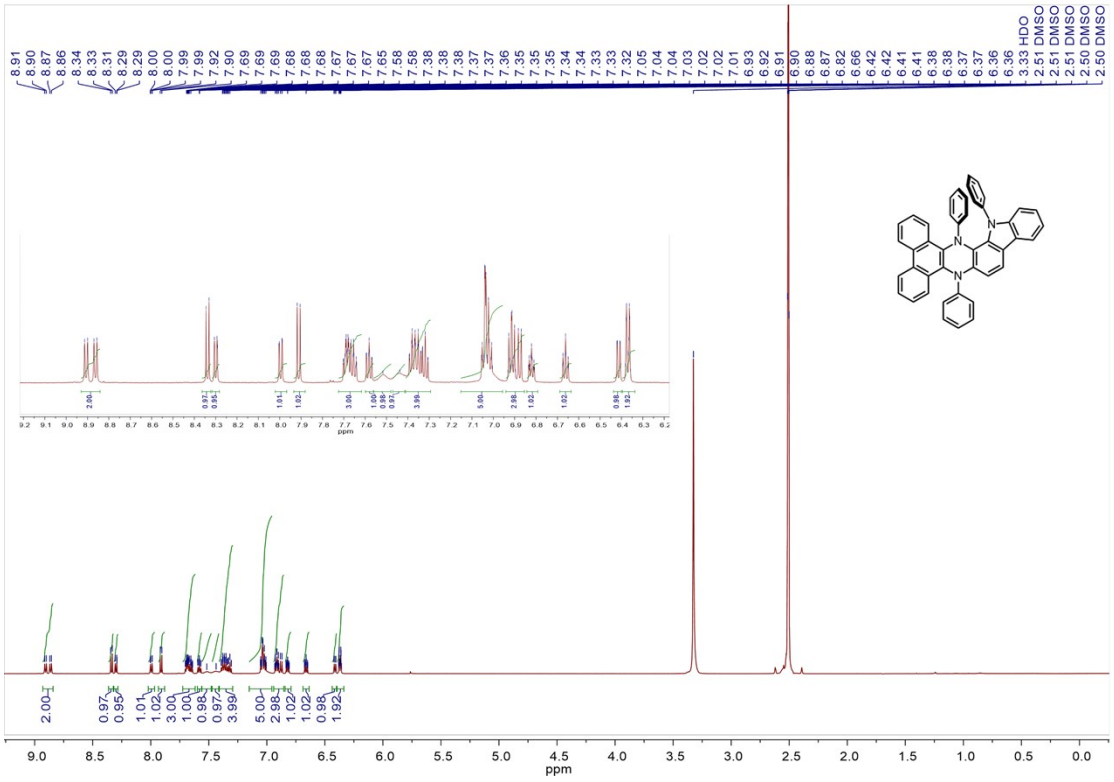

Figure S17. ^{1}H NMR spectrum of **DPAC-*w*-3,4-phCz** (600 MHz, DMSO-d_6, ppm).

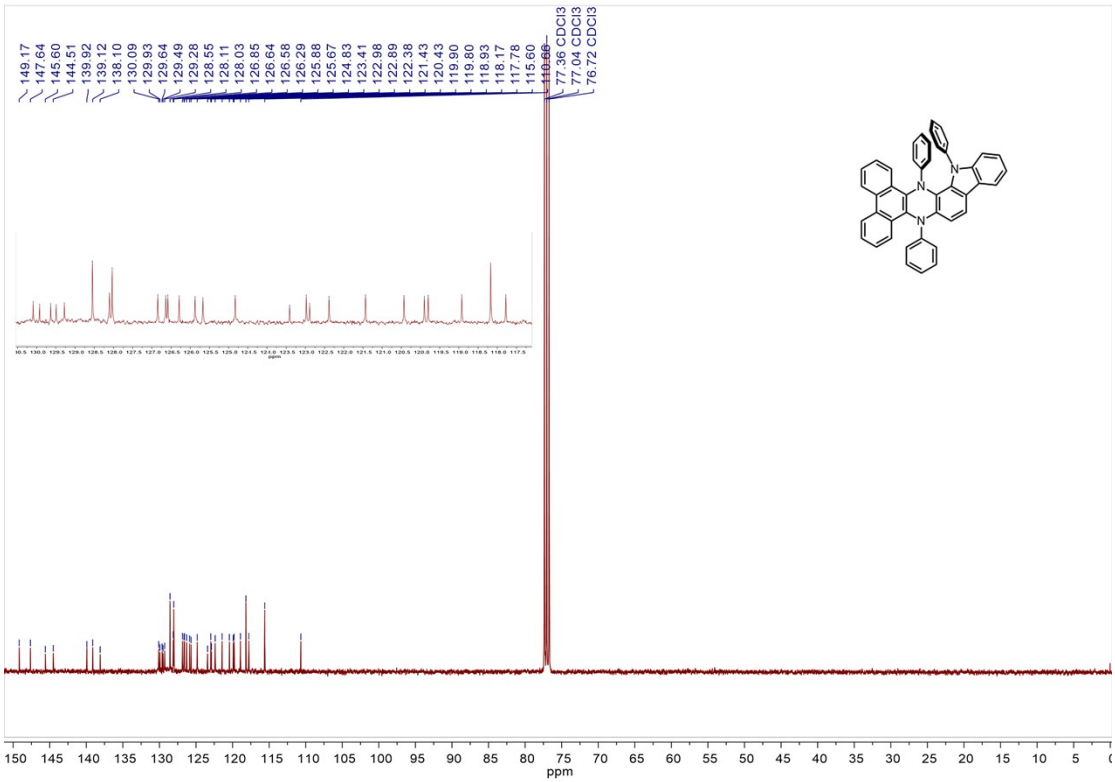

Figure S18. ^{13}C NMR spectrum of **DPAC-*w*-3,4-phCz** (151 MHz, $CDCl_3$-*d*, ppm).

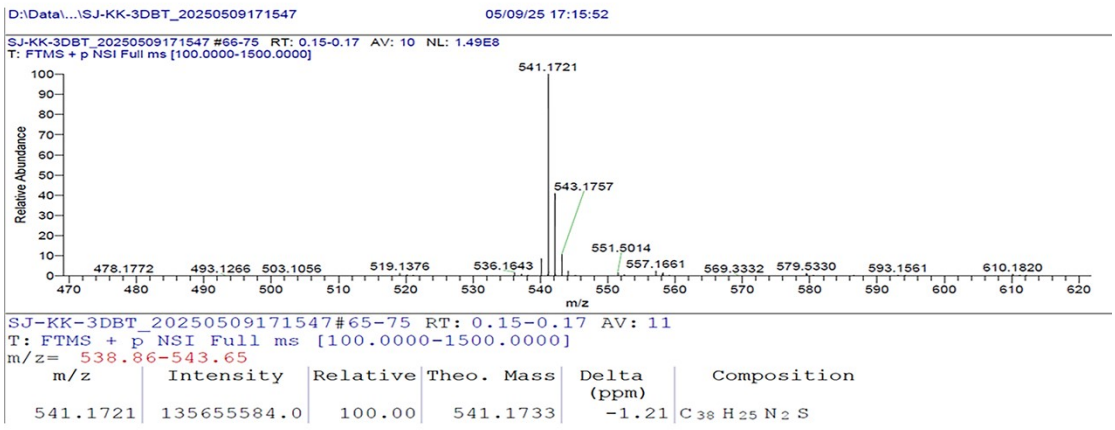

Figure S19. HRMS spectrum of **DPAC-*w*-3,4-DBT**.

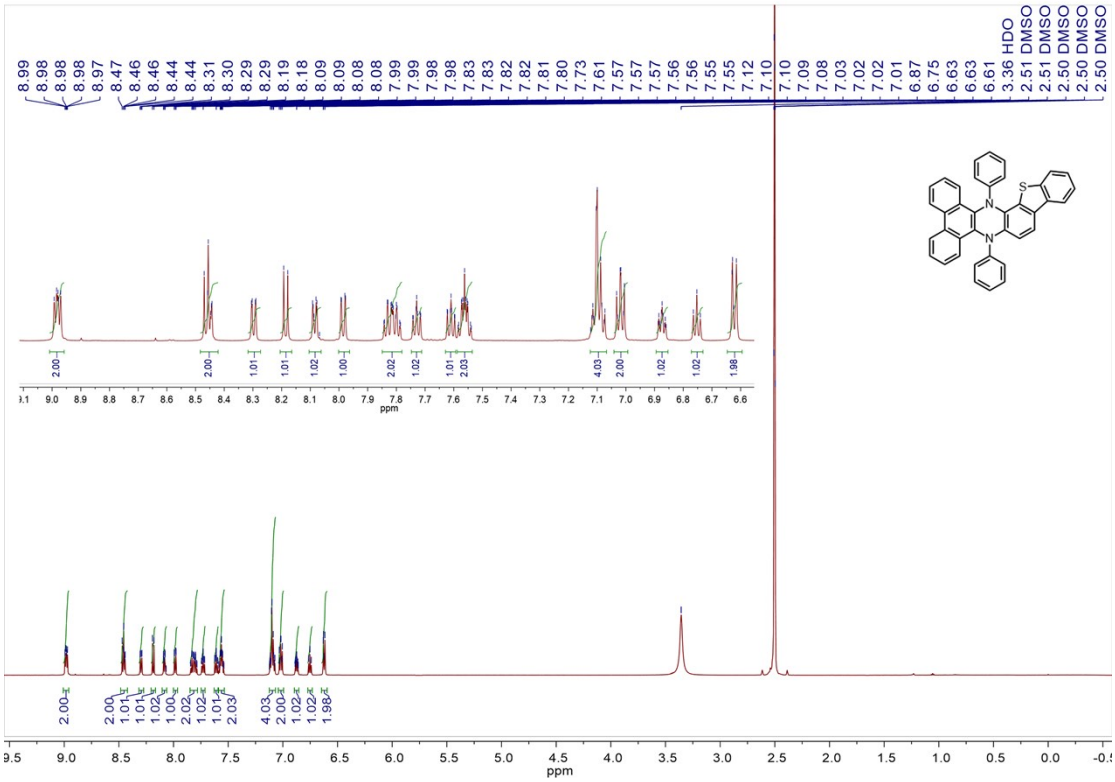

Figure S20. ^{1}H NMR spectrum of **DPAC-*w*-3,4-DBT** (600 MHz, DMSO-d_6, ppm).

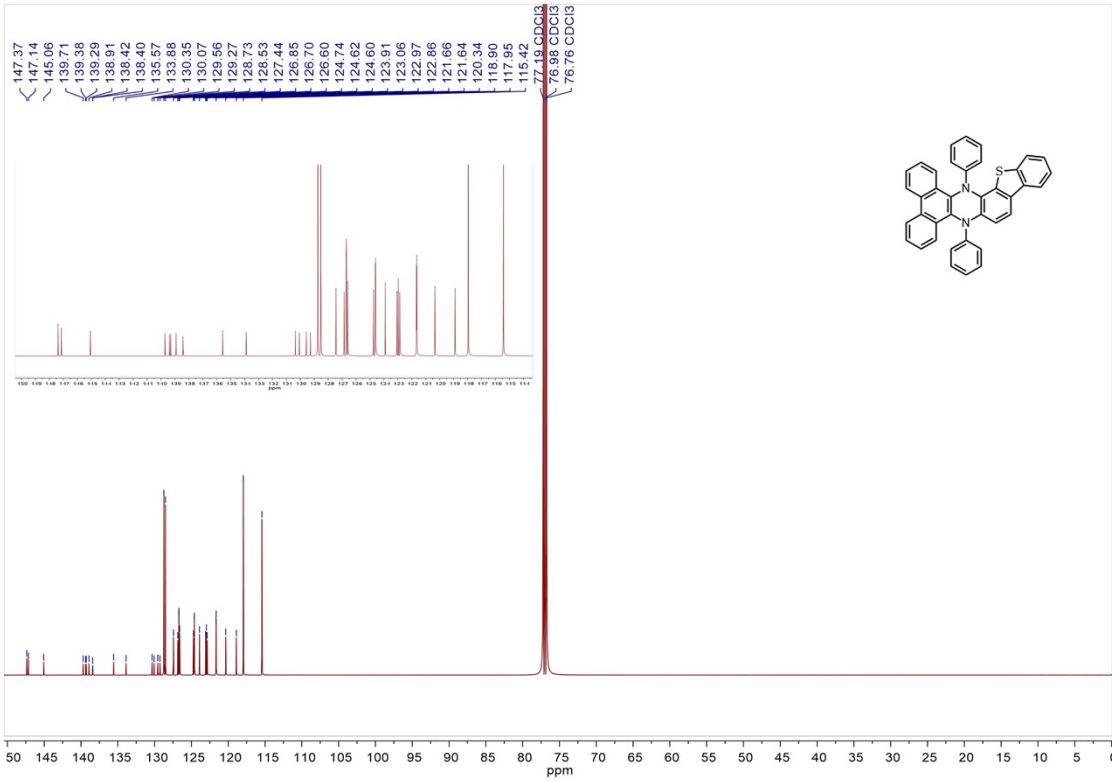

Figure S21. ^{13}C NMR spectrum of **DPAC-*w*-3,4-DBT** (151 MHz, $CDCl_3$-*d*, ppm).

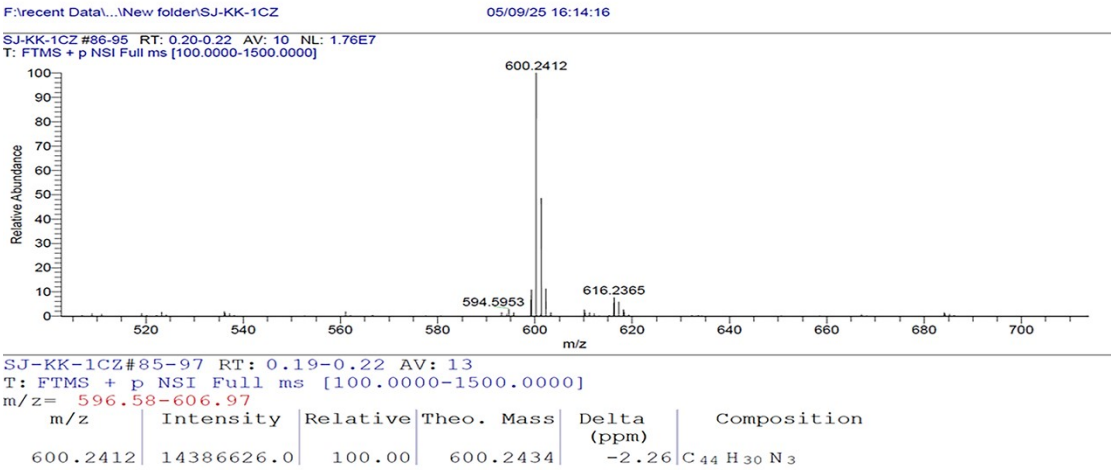

Figure S22. HRMS spectrum of **DPAC-*h*-1-phCz**.

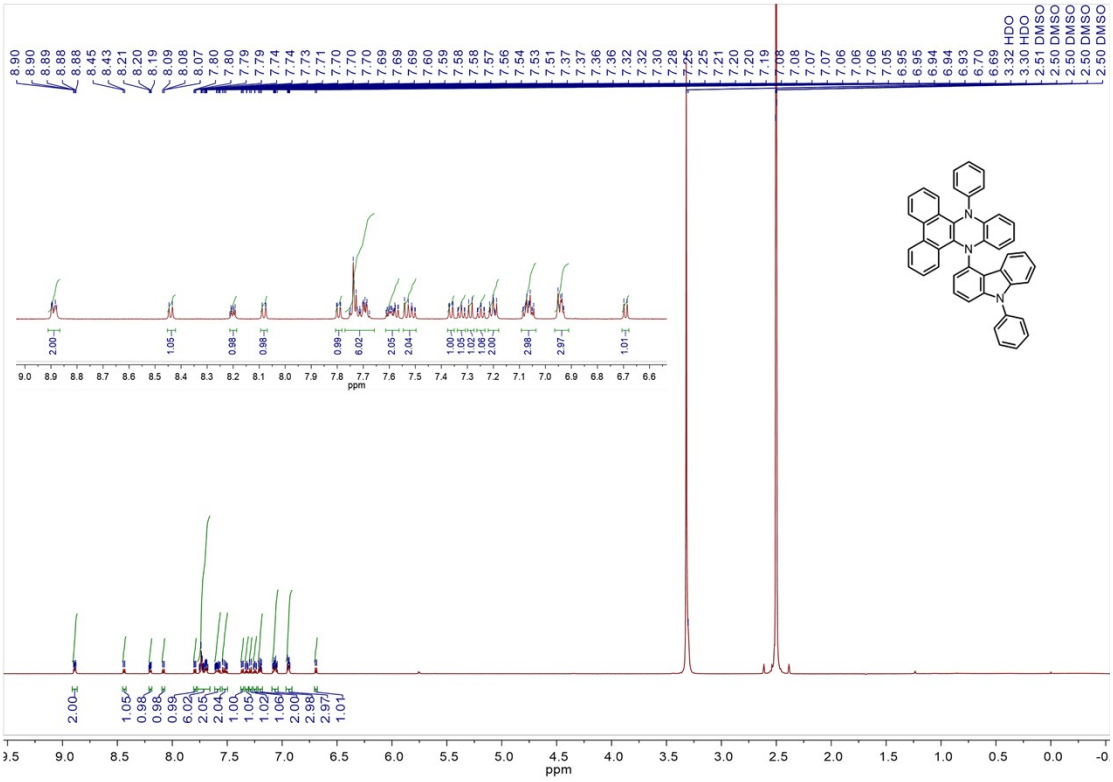

Figure S23. ^{1}H NMR spectrum of **DPAC-*h*-1-phCz** (600 MHz, DMSO-d_6, ppm).

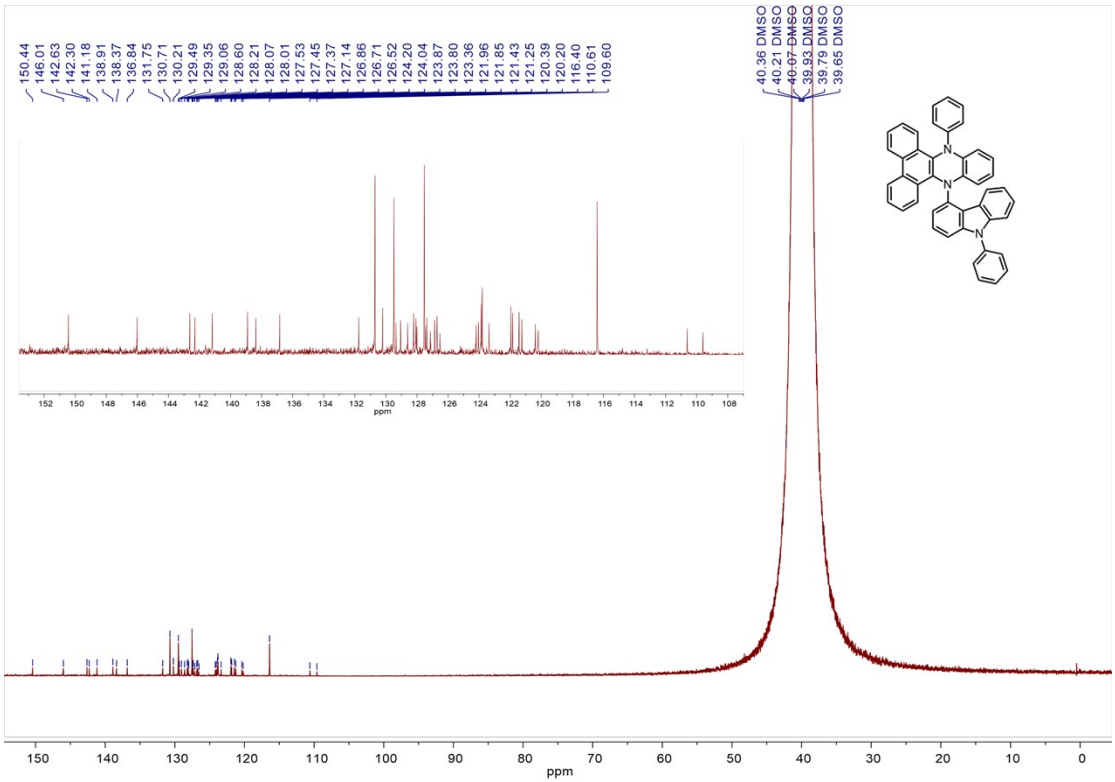

Figure S24. ^{13}C NMR spectrum of **DPAC-*h*-1-phCz** (151 MHz, DMSO-d_6, ppm).

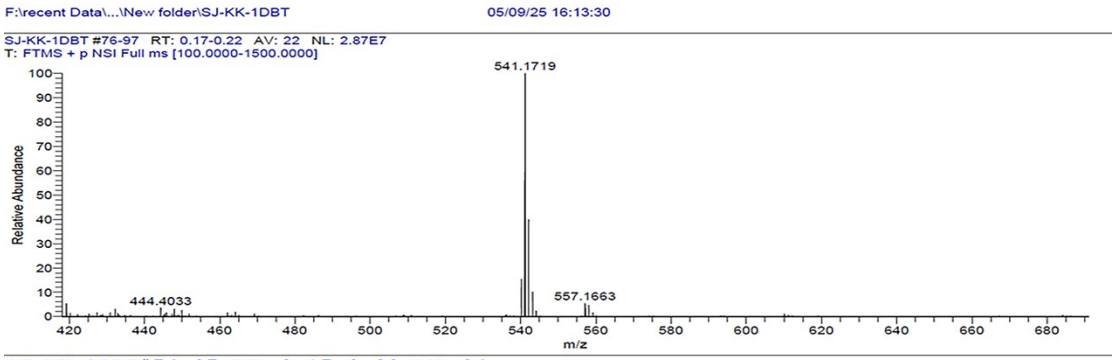

SJ-KK-1DBT#74-97 RT: 0.17-0.22 AV: 24
T: FTMS + p NSI Full ms [100.0000-1500.0000]
m/z= 539.05-555.51

m/z	Intensity	Relative	Theo. Mass	Delta (ppm)	Composition
541.1719	27015766.0	100.00	541.1733	-1.38	$C_{38}H_{25}N_2S$

Figure S25. HRMS spectrum of **DPAC-*h*-1-DBT**.

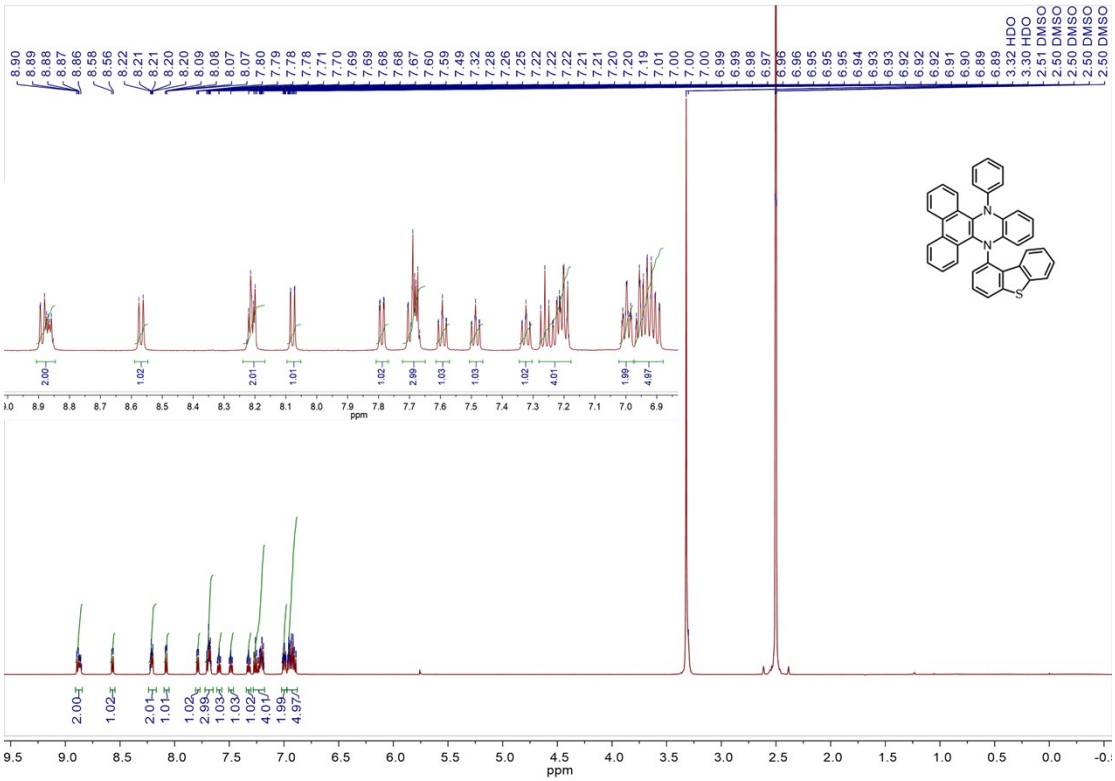

Figure S26. ^{1}H NMR spectrum of **DPAC-*h*-1-DBT** (600 MHz, DMSO-d_6, ppm).

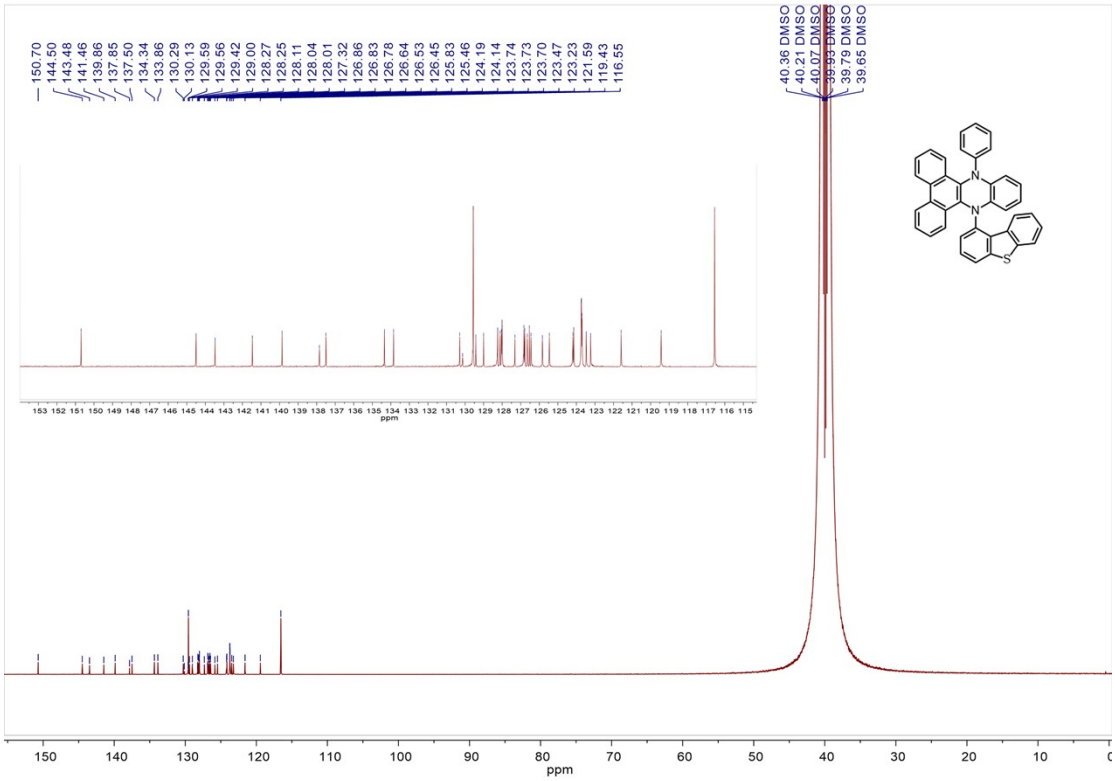

Figure S27. ^{13}C NMR spectrum of **DPAC-*h*-1-DBT** (151 MHz, DMSO-d_6, ppm).

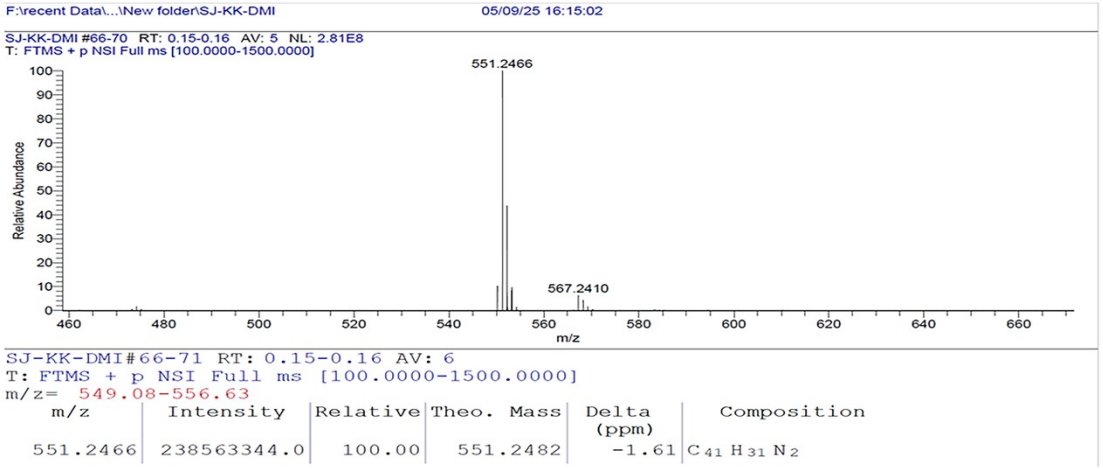

Figure S28. HRMS spectrum of **DPAC-*h*-1-DMI**.

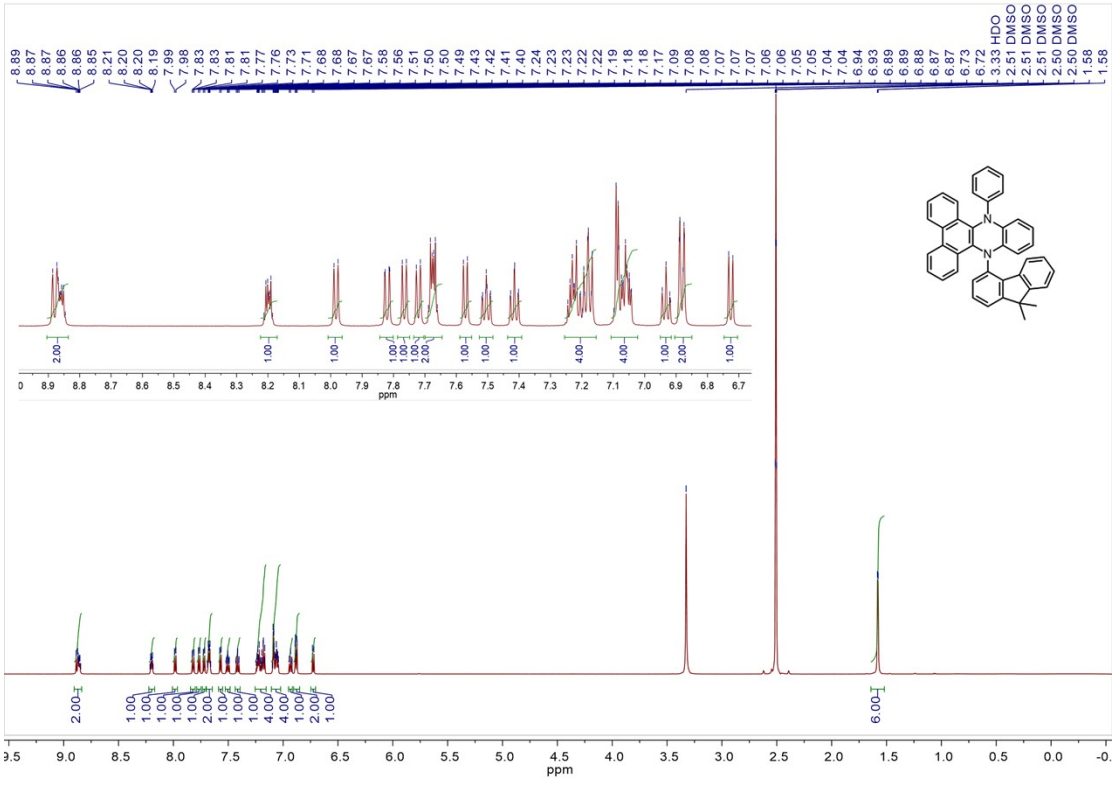

Figure S29. ^{1}H NMR spectrum of **DPAC-*h*-1-DMI** (600 MHz, DMSO-d_6, ppm).

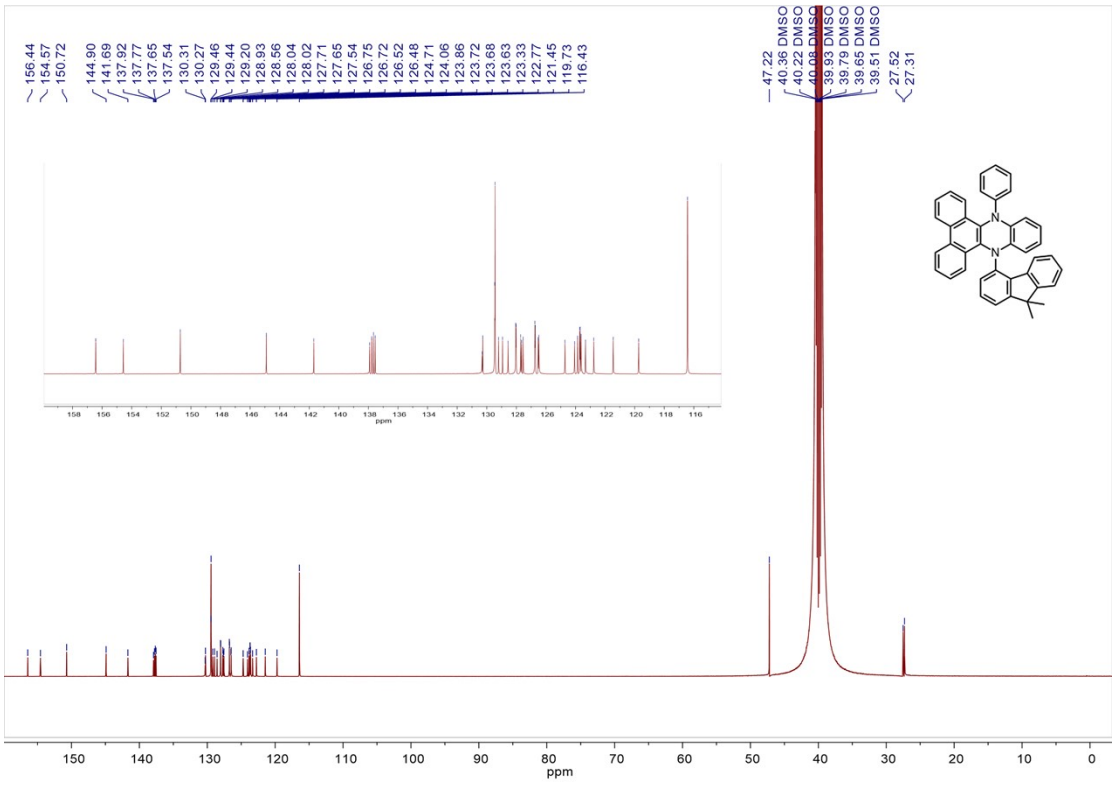

Figure S30. ^{13}C NMR spectrum of **DPAC-*h*-1-DMI** (151 MHz, DMSO-d_6, ppm).

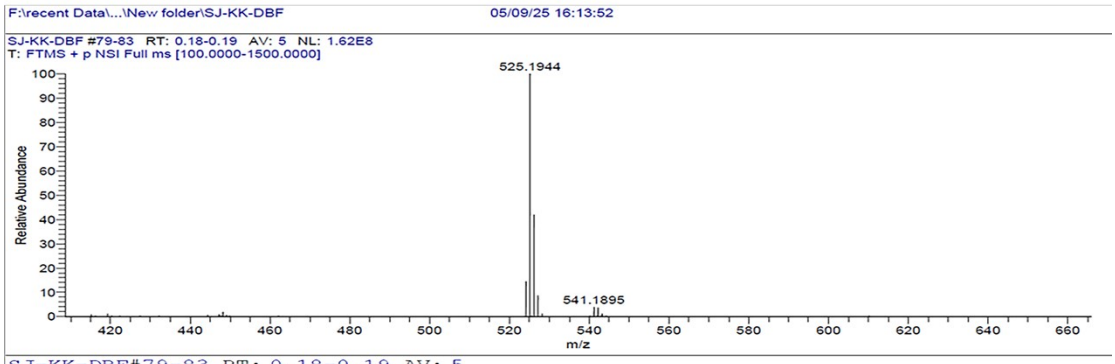

SJ-KK-DBF#79-83 RT: 0.18-0.19 AV: 5
T: FTMS + p NSI Full ms [100.0000-1500.0000]
m/z= 522.97-529.21

m/z	Intensity	Relative	Theo. Mass	Delta (ppm)	Composition
525.1944	167193232.0	100.00	525.1961	-1.72	$C_{38}H_{25}ON_2$

Figure S31. HRMS spectrum of **DPAC-*h*-1-DBF**.

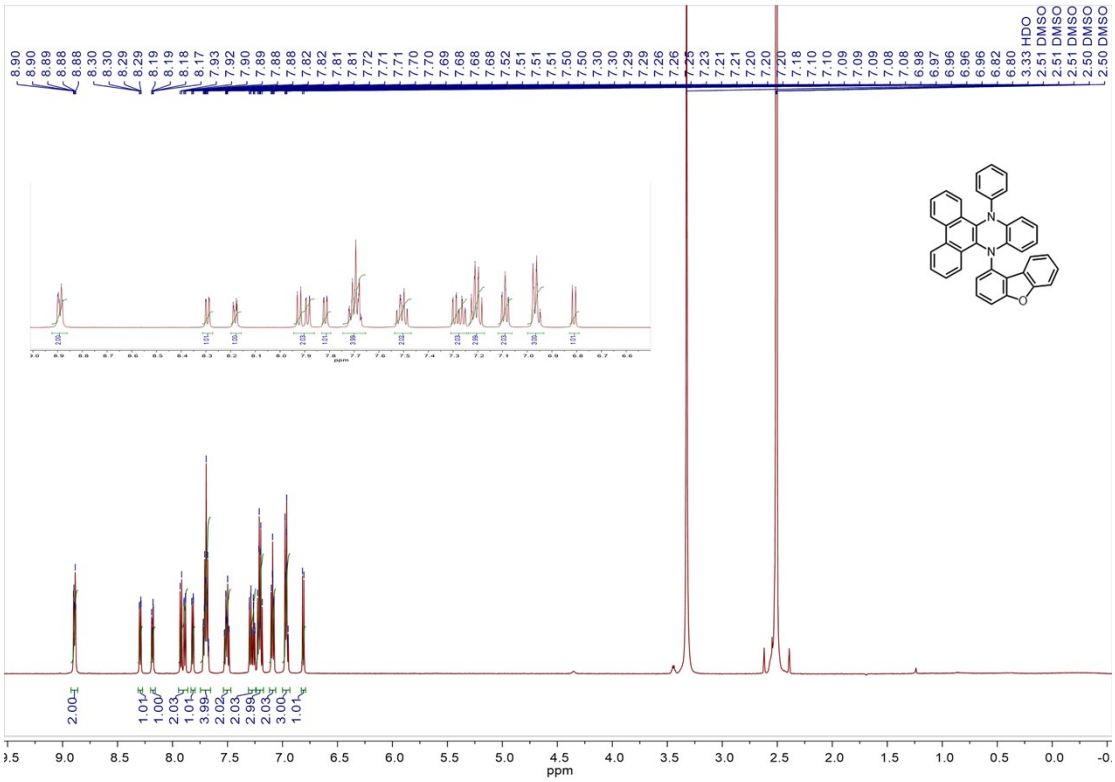

Figure S32. [1]H NMR spectrum of **DPAC-*h*-1-DBF** (600 MHz, DMSO-d_6, ppm).

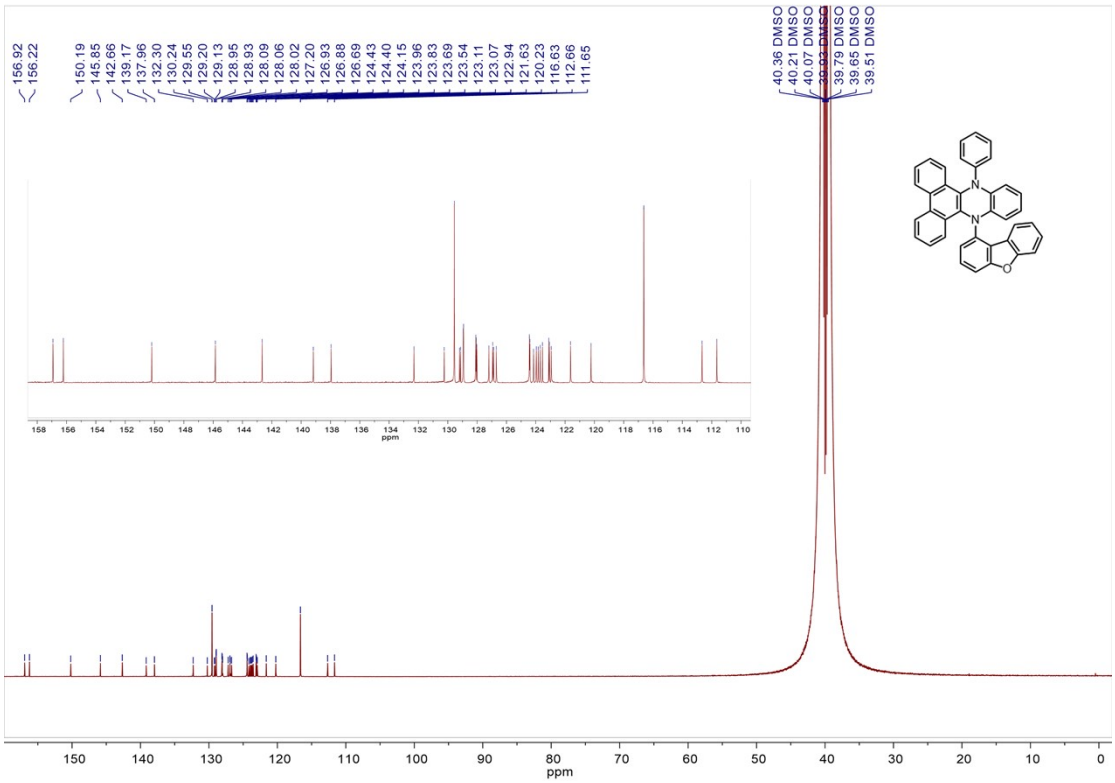

Figure S33. [13]C NMR spectrum of **DPAC-*h*-1-DBF** (151 MHz, DMSO-d_6, ppm).

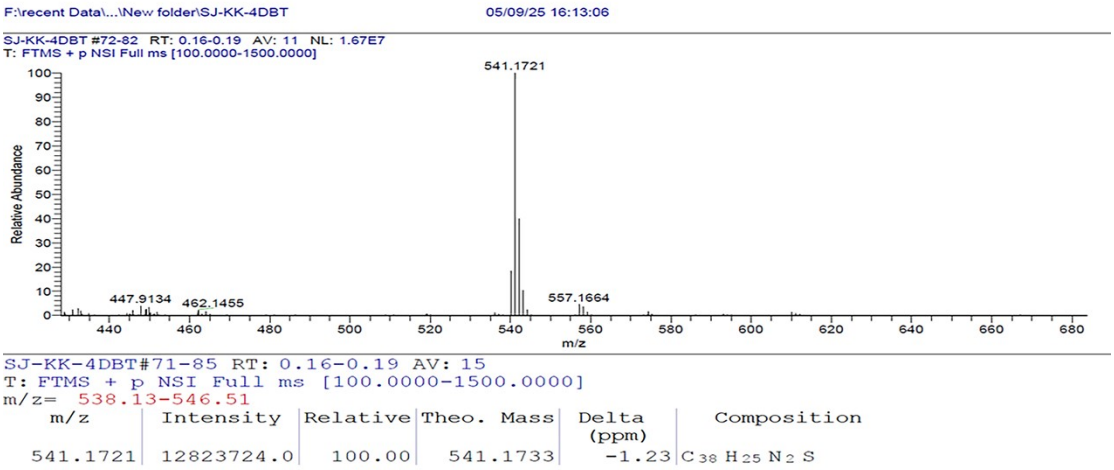

Figure S34. HRMS spectrum of **DPAC-*h*-4-DBT**.

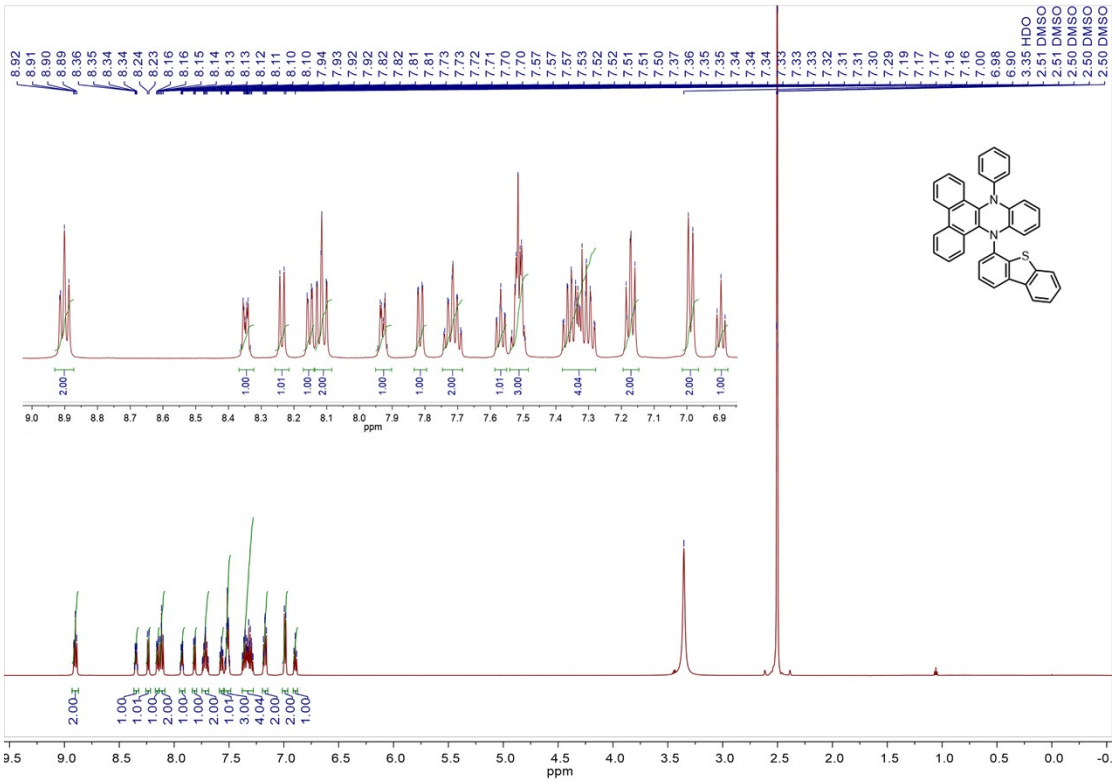

Figure S35. ^{1}H NMR spectrum of **DPAC-*h*-4-DBT** (600 MHz, DMSO-d_6, ppm).

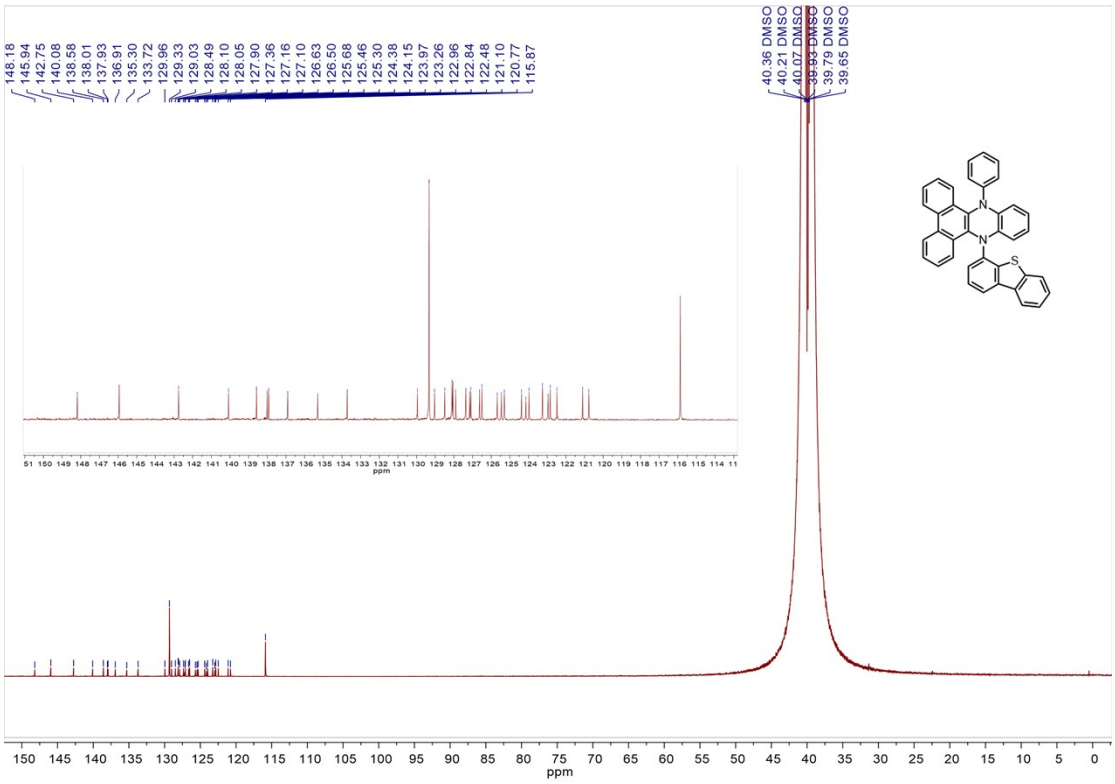

Figure S36. ^{13}C NMR spectrum of **DPAC-*h*-4-DBT** (151 MHz, DMSO-d_6, ppm).

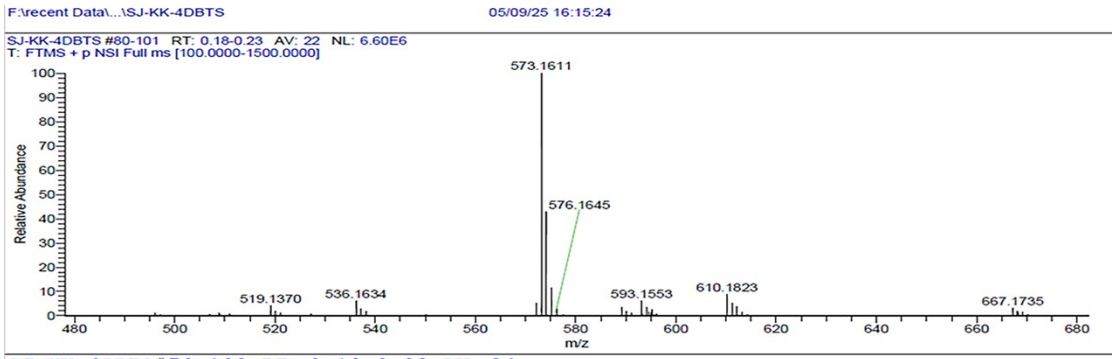

SJ-KK-4DBTS#79-102 RT: 0.18-0.23 AV: 24
T: FTMS + p NSI Full ms [100.0000-1500.0000]
m/z= 570.62-580.39

m/z	Intensity	Relative	Theo. Mass	Delta (ppm)	Composition
573.1611	6554939.0	100.00	573.1631	-1.98	$C_{38}H_{25}O_2N_2S$

Figure S37. HRMS spectrum of **DPAC-*w*-3,4-DBTS**.

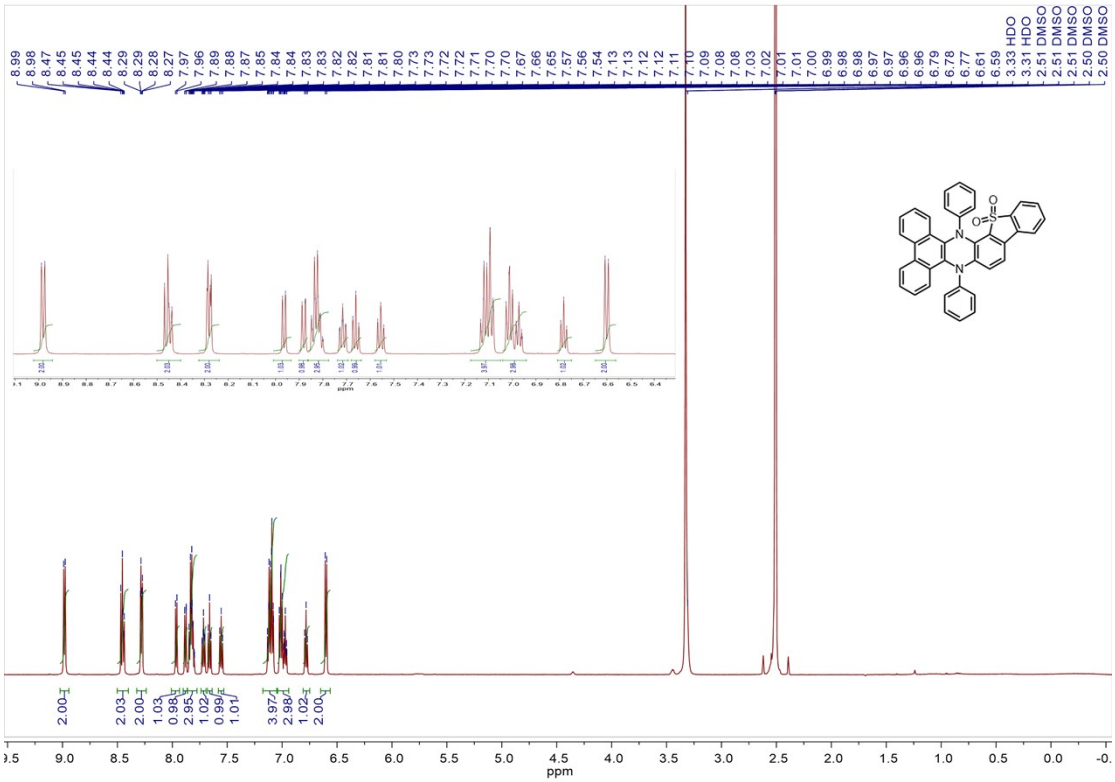

Figure S38. ^{1}H NMR spectrum of **DPAC-*w*-3,4-DBTS** (600 MHz, DMSO-d_6, ppm).

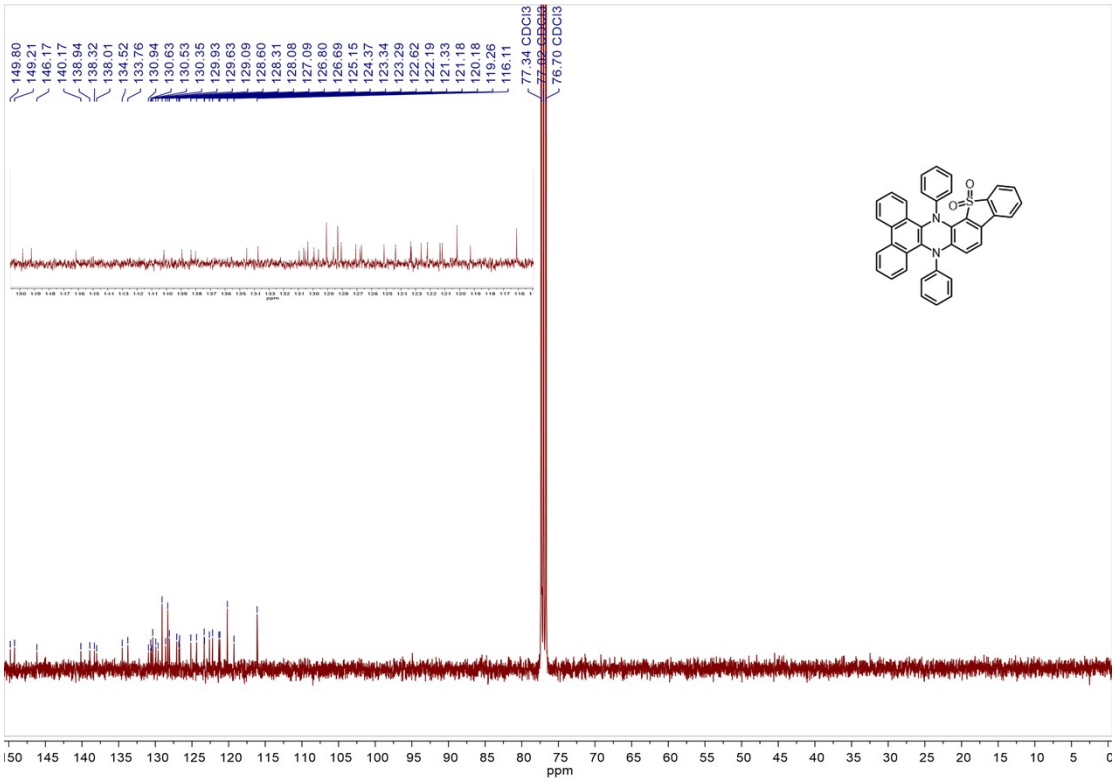

Figure S39. ^{13}C NMR spectrum of **DPAC-*w*-3,4-DBTS** (151 MHz, $CDCl_3$-*d*, ppm).